Construction and Building Materials

# Performance of soils enhanced with eco-friendly biopolymers in unconfined compression strength tests and fatigue loading tests

--Manuscript Draft--

| | |
|---|---|
| **Manuscript Number:** | CONBUILDMAT-D-19-10101R2 |
| **Article Type:** | Research Paper |
| **Keywords:** | Xanthan gum; Initial moisture content; Unconfined compression strength; Repeated loads; Ground improvement |
| **Corresponding Author:** | Xueyu Geng, Ph.D<br>University of Warwick<br>Coventry, UNITED KINGDOM |
| **First Author:** | Jing Ni |
| **Order of Authors:** | Jing Ni |
| | Shanshan Li |
| | Lei Ma |
| | Xueyu Geng, Ph.D |
| **Abstract:** | Recently, biopolymers have emerged in soil stabilisation. The efficiency of biopolymers in ground improvement is mainly dependent on biopolymer types, soil types, biopolymer contents, curing periods, thermal treatment and mixing methods. However, the effect of the initial moisture content during sample preparation stages, on the mechanical behaviours of biopolymer-treated soils, has not been fully understood. The first part of this study probed the role of initial moisture content, in treating Shanghai clay with the xanthan gum by performing standard proctor compaction tests, Atterberg limit tests, unconfined compression strength (UCS) tests and microstructural analysis, while the second part contributed to capture the fatigue behaviours of the samples treated with an ideal moisture content by performing constant-amplitude and stepping-amplitude fatigue loading tests. Our results showed that the improvement appeared to occur from an average optimum moisture content for the treated soils (treated optimum), which was 3% wet of the untreated optimum. As the initial moisture content increased, the UCS values were elevated. However, there existed an ideal initial moisture content leading to the maximum strengthening efficiency. For xanthan gum content (i.e., the mass of xanthan gum with respect to the mass of dry soil) ranging from 1.0% to 5.0%, this ideal value was between 1.1 and 1.2 times the treated optimum. Our results also indicated that xanthan gum, as a biopolymer soil strengthener, was efficient in increasing either fatigue life or bearing capacity, under repeated loading for xanthan gum-soil matrices, when compared to untreated soils. While the untreated soils failed at the stress level of only half the UCS, the xanthan gum-treated soils with a 3.0% xanthan gum content sustained at the end of the tests. These data imply the potential use of xanthan gum in soil stabilisation, under repeated loads. |

# Performance of soils enhanced with eco-friendly biopolymers in unconfined compression strength tests and fatigue loading tests

**Jing Ni[a], Shan-Shan Li[a], Lei Ma[a], Xue-Yu Geng[b,*]**

[a]*Department of Civil Engineering, University of Shanghai for Science and Technology, 200093 Shanghai, P.R. China.*

[b]*School of Engineering, University of Warwick, Coventry, CV4 7AL, UK (*corresponding author)*

***Corresponding author**: Xue-Yu Geng (Email: xueyu.geng@warwick.ac.uk)

**Abstract** Recently, biopolymers have emerged in soil stabilisation. The efficiency of biopolymers in ground improvement is mainly dependent on biopolymer types, soil types, biopolymer contents, curing periods, thermal treatment and mixing methods. However, the effect of the initial moisture content during sample preparation stages, on the mechanical behaviours of biopolymer-treated soils, has not been fully understood. The first part of this study probed the role of initial moisture content, in treating Shanghai clay with the xanthan gum by performing standard proctor compaction tests, Atterberg limit tests, unconfined compression strength (UCS) tests and microstructural analysis, while the second part contributed to capture the fatigue behaviours of the samples treated with an ideal moisture content by performing constant-amplitude and stepping-amplitude fatigue loading tests. Our results showed that the improvement appeared to occur from an average optimum moisture content for the treated soils (treated optimum), which was 3% wet of the untreated optimum. As the initial moisture content increased, the UCS values were elevated. However, there existed an ideal initial moisture content leading to the maximum strengthening efficiency. For xanthan gum content (i.e., the mass of xanthan gum with respect to the mass of dry soil) ranging from 1.0% to 5.0%, this ideal value was between 1.1 and 1.2 times the treated optimum. Our results also indicated that xanthan gum, as a biopolymer soil strengthener, was efficient in increasing either fatigue life or bearing capacity, under repeated loading for xanthan gum-soil matrices, when compared to untreated soils. While the untreated soils failed at the stress level of only half the UCS, the xanthan gum-treated soils with a 3.0% xanthan gum content sustained at the end of the tests. These data imply the potential use of xanthan gum in soil stabilisation, under repeated loads.

**Keywords** Xanthan gum, Initial moisture content, Unconfined compression strength, Repeated loads, Ground improvement

## 1. Introduction

During the past two decades, the application of biological processes to soil stabilisation has emerged in geotechnical engineering [1, 2]. Bio-mineralisation, which leads to mineral precipitation using the bio-technological mediation route, has been extensively investigated as a bio-treatment for soils [3-8]. More recently, the direct use of biogenic excrement (i.e., biopolymers) as a ground improvement method has gained increased academic interest, as biopolymers are abundant in nature and are considered eco-friendly materials for soil treatment [9], and on the other hand able to improve soil strength, even under a very low biopolymer-to-soil ratio (e.g., 0.5%) [10-12].

As a commonly applied contemporary biopolymer type in various practices, polysaccharides have been evaluated for their capacity to treat soils. Beta-glucan ($\beta$-1, 3/1, 6-glucan) and guar gum have been found operational and effective in enhancing the mechanical strength of soils [13, 14]. Gellan gum and agar gum have similar properties, including thermos-gelation and significant efficiency in strengthening soils [15-19]. The application of carrageenan and chitosan as additives to earthen constructions contributes positively on water durability [20-22]. In addition to polysaccharides, the incorporation of protein-based biopolymers (e.g., casein and sodium caseinate salt) to improve the mechanical properties and durability of natural soils has also been reported [23, 24].

Throughout the literature, it has been recognized that the efficiency of biopolymers in ground improvement is mainly dependent on biopolymer types, soil types, biopolymer contents, curing periods, thermal treatment and mixing methods. The effect of the moisture content on the performance of biopolymer-treated soils, however, has not been fully understood. Some researchers have revealed that the biopolymer-treated soils [12, 24], like other geopolymer-treated soils [25], appear to have a higher mechanical strength with a lower value of moisture content. During the sample preparation stage, a reduction in the initial moisture content may lead to an increased strength [19], which is illustrated in Fig. 1 (Zone

*A*). However, the strength is unlikely to continue increasing when the initial moisture content decreases (Fig. 1, Zone *C*), as too little water results in a poorly dissolved biopolymer solution, which could adversely affect the workability of the biopolymer-soil matrix and its consequent mechanical strength [26]. As a result, there might exist an ideal initial moisture content ($w_I$) leading to the highest strength as illustrated in Fig. 1, i.e., inflection point from Zone *B* to Zone *A*. Therefore, the initial moisture content appears to play an important role in the efficiency of soil treatment. Up to now, little research has been performed in this area. Usually, the initial moisture content has been set as a fixed value, e.g., liquid limit [13, 16, 26], optimum moisture content [21, 23], and natural moisture content [27].

In this study, the effect of the initial moisture content on the efficiency of soil treatment will be probed by an experimental study on the xanthan gum-treated Shanghai clay. Xanthan gum has been extensively researched in the soil treatment due to its unique functional properties. It has excellent cold water dissolving capacity, pH stability, storage stability, ionic salt compatibility, and pseudo-plastic flow characteristics [28, 29]. For geotechnical engineering, xanthan gum has been used as polymer support fluids to stabilize deep excavations [30, 31]. Recent studies have reported that xanthan gum, providing bonds between soil particles, has the potential to act as a soil strengthener [12, 14, 26, 27]. In addition, the presence of xanthan gum in soils reduces the hydraulic conductivity due to the "clogging effect", and enables hydrogen bonds to enhance the strength and corrosion resistance of sands [14, 26, 27].

On the other hand, xanthan gum are available at reasonable prices. In general, the market prices of biopolymers are more expensive than conventional soil stabilizers and inorganic binders (e.g., geopolymers). However, taken into account the global greenhouse gas reduction efforts (e.g., carbon emission trading), biopolymers will become remarkably competitive in soil treatment, e.g., for a unit amount (1 ton) of soil treatment, 0.5% xanthan gum is only 3.6% more expensive than 10% cement [9, 32]. In addition, the biopolymers have higher production

costs due to their widespread use in the fields of food production, agriculture, and medical treatment. For geotechnical applications, it is expected that the price of biopolymers will be greatly reduced due to the unnecessary edible standards [9, 14].

To the authors' knowledge, limited research has accessed the fatigue behaviours of the xanthan gum-treated soils. Soils subjected to repeated loads can fail under a stress level consisting only a fraction of a static strength [33-38]. Therefore, a lack of understanding of the mechanical behaviours of the biopolymer-treated soils under fatigue loading will restrict the evaluation of their long-term resilience and practical engineering performances (e.g., highway pavements, railway tracks, and airport runways). Given this background, this study involved investigating the performances of xanthan gum-treated soils from two aspects, i.e., the ideal treatment condition (e.g., ideal initial moisture content) to achieve the maximum strengthening effect and fatigue behaviours under the ideal treatment condition. Standard proctor compaction tests and Atterberg limit tests were also performed along with the SEM images to better understand the underlying strengthening mechanisms.

## 2. Materials and Methods

### *2.1. Shanghai clay*

Shanghai lies in the Yangtze River delta alluvial plain in China. For this study, natural soils were sampled from a construction site of Metro Line 15 in the northwest Shanghai, at a depth of 8.9 m. Table 1 shows some of the basic engineering properties for Shanghai clay, e.g., optimum moisture content (OMC) and maximum dry density ($\rho_{dmax}$), and gravimetric-volumetric parameters.

Particle size distribution analysis was performed on the soil using a Mastersizer 3000 particle size analyser (Malvern, UK), which caters for the particles in the range of 10 nm to 3.5 mm. As shown in Fig. 2, the natural soil had 33.41% by weight sand content, 54.86% silt

content, and 11.73% clay content based on the soil particle size ranges as recommended in ASTM D422. The Atterberg limits, i.e., the liquid and plastic limits of the natural soil, were found to be $w_L$=37.9% and $w_P$=22%, respectively. The corresponding plastic index was $I_P$=15.9%. Combined with the particle size distribution curve and Atterberg limits, the natural soil was therefore classified as sand lean clay, as per ASTM D2487.

An X-ray fluorescence (XRF) test on the soil was performed using a portable QUANTAX energy-dispersive X-ray microanalysis (EDX) spectrometer (Brucker, Germany), equipped with a 2.5 kg probe, 50 W pulse processor and Esprit analysis software. The XRF spectrum (Fig. 3) indicated that the most abundant elements were Si, C, O, Al, K, Mg, Na, and Fe.

Mineralogical analysis of the natural soil was conducted using the X-ray powder diffraction test (XRPD), using a D8 ADVANCE diffractometer (Brucker, Germany). Data was automatically collected for phase angles ($2\theta$), ranging between 5º and 90º, at 0.02º intervals. Identification of the crystalline phases was carried out using JADE software. XRPD patterns are shown in Fig. 4, including main peak identification, $SiO_2$.

### *2.2. Xanthan gum*

Xanthan gum is a polysaccharide formed by the fermentation of sugar (e.g., glucose or sucrose) by the bacterium *Xanthomonas campestris.* It was chosen to treat Shanghai clay for its unique functional properties and reasonable prices as previously demonstrated. The xanthan gum powder for this study was manufactured by Shandong Fengtai Biological Technology Co., Ltd..

### *2.3. Sample fabrication*

Sample preparation for both unconfined compression strength tests and fatigue loading tests followed the same procedures. The Shanghai clay was oven dried (105 ºC) for 24 hours,

broken down carefully with rubber hammers, and sieved using a 2 mm sieve to obtain a base soil. The base soil was thoroughly mixed with xanthan gum, before distilled water was added. To increase the solubility, the distilled water was heated to 80 ºC [26]. A metal trowel was used for mixing manually for about five minutes until a homogeneous xanthan gum-soil mixture was obtained. The mixture was then placed inside a cylindrical mould with an inner diameter of 39.1 mm and a height of 80 mm in three layers. For each layer, 25 blows were applied through a rammer (305.5 g) dropping from a height of 247 mm. The compacted samples were extruded after compaction, and cured in a controlled environment at 60% relative humidity and 20 ºC for 28 days.

### 2.4 *Experimental programme*

The experimental program involved exploring the influence of using xanthan gum on the behaviours of Shanghai clay from five aspects: (1) compaction properties; (2) Atterberg limits; (3) microscopic structures; (4) mechanical properties under unconfined compression and (5) fatigue loading. The following subsections present the test procedures for each component of the experimental programme. Each test was replicated at least three times to achieve a reliable average.

#### *2.4.1* Standard proctor compaction tests

The standard proctor compaction tests were conducted in accordance with ASTM D698 to determine the maximum dry density and its corresponding optimum moisture content for xanthan gum-treated soil samples. Five xanthan gum contents (the mass of xanthan gum with respect to the mass of dry soil), e.g., $m_b/m_s$=1.0%, 2.0%, 3.0%, 4.0%, and 5.0% (Table 2), were used to investigate the variation of compaction properties with the increasing xanthan gum content.

#### *2.4.2* Atterberg limit tests

The Atterberg limits ($w_P$ and $w_L$) of the soils treated with five xanthan gum contents (Table 2) were determined by Liquid-Plastic Limit Combined Test (GB/T 50123-2019, Part 9) by using a cone with a mass of 76 g and a tip angle of 30°. The penetration depth of the cone into the sample (55 mm diameter and 40 mm height) was measured 5 s after the cone had been released. For each biopolymer content, the test was repeated on five samples with an increased moisture content. The water contents corresponding to 17 mm and 2 mm determined with the aid of a linear fitting curve in the semi-log plane of cone penetration-moisture content were regarded as liquid limit and plastic limit, respectively.

### *2.4.3.* Unconfined compression strength tests

The effectiveness of incorporating xanthan gum in improving the soil strength at different initial moisture contents was investigated by the unconfined compression strength tests, which were conducted under the strain-controlled condition at a loading rate of 1.5%/min in accordance with ASTM D2166. The xanthan gum contents used were the same as those adopted for the standard proctor compaction and Atterberg limit tests. For each biopolymer content, five initial moisture contents were employed (Table 2). As suggested by Fatehi et al. [23] and Hataf et al. [21], the optimum moisture content of the untreated soil ($w$=23%) (hereafter referred as untreated optimum) was adopted as the minimum initial moisture content. The xanthan gum-treated soil samples with $w$=23% had a lot of voids on the sample surfaces, indicating an unthorough mixing due to the poor workability of the xanthan gum-soil mixture. Then 3% wet of the untreated optimum was selected based on the results of the standard proctor compaction tests (section 2.4.1), which indicated that the mean value of the optimum moisture contents of the treated soils (hereafter referred as treated optimum) with various xanthan gum contents was $w$=26%. Afterwards, the initial moisture content was increased at an interval of 2%. With the increment in the amount of water for sample mixing, the workability of the xanthan gum-soil mixture was improved. However, as the initial moisture content reached 34%, the compacted samples were visually deformed after they

were extruded from the cylindrical mould. Therefore, $w$=32% was adopted as the maximum initial moisture content. The untreated soil sample, prepared with the optimum moisture content $w$=23%, served as a control sample.

### *2.4.4. Fatigue loading tests*

Apart from the unconfined compression strength tests, fatigue loading tests were performed on the xanthan gum-treated soil samples as well. These samples used $w$=30%, and $m_b/m_s$ = 1.0%, 2.0%, and 3.0%. They were cured under the controlled conditions for 28 days before being exposed to the fatigue loading tests. The ZWICK-100HFP5100 test apparatus (ZwickRoell, Germany) was employed to apply fatigue loads. For detailed descriptions see Chen et al. [39-41]. The test procedure started with the mounting of cylindrical samples on the loading frame and bringing the load cell into contact with the sample surface. Through the user-friendly visualisation window, the mean stress, stress amplitude, and maximum loading cycles were fed into the load application device. The loading system was switched on at the same time as the automatic data acquisition system, and fatigue loading was initiated. The process continued until failure of the sample, or the maximum loading cycle was reached.

In this study, the fatigue loading tests involved two strategies: constant-amplitude and stepping-amplitude. In the constant-amplitude tests, the mean stress ($\sigma_m$) and stress amplitude ($\sigma_a$) for each sample remained constant during the loading process. In the stepping-amplitude tests, the mean stress remained constant, but the stress amplitude increased stepwise. Details of the two components of fatigue loading test are described as follows.

The loading schemes for the constant-amplitude and stepping-amplitude fatigue loading tests are shown in Fig. 5. The test input parameters included the mean stress($\sigma_m$) and stress amplitude ($\sigma_a$). The corresponding maximum stress ($\sigma_{max}=\sigma_m+\sigma_a$) and the minimum stress ($\sigma_{min}=\sigma_m-\sigma_a$) were calculated. The effects of $\sigma_m$, $\sigma_a$ and their combination on fatigue life were investigated. The test matrix of constant-amplitude fatigue loading tests is given in Table 3.

The maximum stress were from 1/2 to 3/4 fractions of UCS values referring to Lekha et al. [42], corresponding to medium to high stress levels. The UCS for each treatment condition was used as a basis for the calculation of fatigue stresses (e.g., $\sigma_m$, $\sigma_a$, $\sigma_{max}$, and $\sigma_{min}$). The maximum number of loading cycles for each test was set as 2,000,000. The loading frequency was set as a resonant frequency between the sample and the apparatus, which was about 40 to 45 Hz, rather than a fixed value.

For the stepping-amplitude fatigue loading tests, the mean stress ($\sigma_m$) for each sample was constant, while the stress amplitude ($\sigma_a$) increased step by step, at a constant interval. For each loading step, 500,000 cycles of fatigue loading were applied. The fatigue loading tests started from the first step and stopped until either the designed number of cycles was reached, or the sample failed. The test matrix of the stepping-amplitude fatigue loading tests are given in Table 4.

#### *2.4.5. Microscopic structures*

Scanning electrons microscope (SEM) and field emission scanning electron microscope (FESEM) have been used to explore the microstructural characteristics of biopolymer-treated soils, including shapes, sizes, and aggregation of soil particles [19, 23, 27]. In this study, SEM images were taken for both untreated soils and xanthan gum-treated soils ($m_b/m_s$=1.5% and $w$=28%). Microstructural analysis was conducted to better understand the connection between xanthan gum and Shanghai clay, and furthermore the underlying mechanisms of soil stabilization.

## *3. Results and discussion*

### *3.1 Effect of biopolymer contents on compaction characteristics*

The introduction of xanthan gum altered the compaction characteristics of Shanghai clay. The optimum moisture content was observed to increase from 23% to 26.7%. and the

maximum dry density had a descending trend falling from 1.59 g/cm$^3$ to 1.51 g/cm$^3$, as the xanthan gum content increased from $m_b/m_s$= 0.0% to 5.0% (Fig. 6). Ayeldeen et al. [14] reported that this alteration may depend on both the biopolymer characteristics (e.g., chemical properties and solution viscosities) and soil fine-grained content. In the current study, xanthan gum molecules contain a large number of hydrophilic groups (e.g., -OH and -COOH) and therefore have a large capacity to attract water molecules or dissolve in water, and retain water. As a result, elevating the xanthan gum content increased the amount of absorbed water, and therefore increased the optimum moisture content and decreased the maximum dry density.

### *3.2 Effect of biopolymer contents on Atterberg limits*

The liquid limit increased obviously from 37.9% to 44.9% as the $m_b/m_s$ ratio increased from 0.0% to 1.0%, and then slightly increased with the increasing xanthan gum content, to a maximum value of 51.1% at $m_b/m_s$= 5.0%, as shown in Fig. 7. The increasing trend of liquid limit of xanthan gum-soil matrix was also observed by Chang et al. [43]. The mechanism responsible for this phenomenon is similar to that works in compacting xanthan gum-treated soil (e.g., hydrophilic properties and water retention capacity). Treated samples with a higher xanthan gum content had a higher content of hydrophilic xanthan gum hydrogel, leading to a higher liquid limit. Simultaneously, the plastic limit increased gradually from 22% to 25.7% as the xanthan gum content increased from 0.0% to 5.0%.

### *3.3. Results of unconfined compression strength tests*

#### *3.3.1 Effect of initial moisture content on Stress-strain behaviour*

The typical stress-strain curves for five xanthan gum contents at an initial moisture content $w$=30% are shown in Fig. 8. The trends of axial stress versus axial strain of xanthan gum-treated soil samples differed gradually from that of the untreated soil sample ($m_b/m_s$=

0.0%) with the increasing $m_b/m_s$ ratio, indicating that adding xanthan gum to soils provided strengthening effects. On the other hand, the xanthan gum-treated soil samples were more deformable, i.e., the peak axial strain corresponding to the peak axial stress increased from 1.67% to 5.12% as the xanthan gum content increased from 0.0% to 5.0%.

When the initial moisture content was reduced to the treated optimum $w$=26%, the xanthan gum-treated soils also had improved stress-strain behaviours (Fig. 9), however, not as prominent as those for 30% initial moisture content. This implies that using the treated optimum as an initial moisture content did not necessarily lead to the best strengthening effect. This may be due to the undesirable workability caused by insufficient water for xanthan gum-soil matrix mixing. As described in the previous section 3.2, the plastic limit of the xanthan gum-soil matrix increased as a result of increasing the xanthan gum content. Therefore, the initial moisture content of 26% was slightly larger than the plastic limit of the soil samples after they had been treated with xanthan gum at $m_b/m_s$ ratio ranging from 1.0 to 5.0% ($w_p$= 23.5 to 25.7%).

The moisture-dependent stress-strain behaviour is further illustrated in Fig. 10. For a given value of $m_b/m_s$= 1.0%, the efficiency of xanthan gum in improving the soil mechanical behaviour was intimately related to the initial moisture content. Four of the five stress-strain curves for xanthan gum-treated soils lie above the untreated soil, indicating the strengthening effect can only be obtained for a moisture content larger than 26% (treated optimum). The treated samples prepared with the untreated optimum (23%) seemed not to differ from the untreated sample. The similar phenomenon was also observed for $m_b/m_s$ = 2.0% prepared with the untreated optimum. This could be explainable that $w$=23% was even smaller than the plastic limit of the xanthan gum-treated soils, which resulted in an unthorough mixing and prevented the xanthan gum to be an efficient binder. In addition, the strength was observed to reach a maximum value of 3.47 MPa at the initial water content $w$=30%, where either a smaller value $w$=28% or a larger value $w$=32% resulted in a reduced peak axial stress. This

phenomenon indicates that there exists an ideal initial moisture content that can lead to a maximum strengthening effect.

### *3.3.2 Effect of initial moisture content on UCS*

The variation of the unconfined compression strength (UCS) defined as the peak axial stress, with an increasing initial moisture content for untreated soils are shown in Fig. 11. The UCS underwent an increase and then a decrease as the initial moisture content increased from 17% to 30% with a peak value of 1.98 MPa at the optimum moisture content $w$=23%.

Figure 12 shows the trends of UCS with an increasing moisture content for five biopolymer contents. For a given value of $m_b/m_s$=1.0%, the UCS initially increased from 2.67 MPa to a peak value of 3.42 MPa as the initial moisture content increased from 26% to 30%. Afterwards, additional amount of water led to a reduced UCS value of 2.98 MPa. This trend retained when $m_b/m_s$ =1.0% was replaced with $m_b/m_s$ =4.0% and 5.0%. For $m_b/m_s$= 2.0% and 3.0%, the UCS values also underwent an increment and a decrement with the increasing moisture content, but the peak value of UCS was observed at $w$=28%.

The overall trend of UCS indicate that xanthan gum-treated soil samples with all five biopolymer contents grained strength as the moisture content increased from 26% to 28%. Further elevating the moisture content from 28% to 30% led to an increased UCS for $m_b/m_s$ =1.0%, 4.0% and 5.0% and a decreased UCS for $m_b/m_s$ =2.0% and 3.0%. Afterwards, as the moisture content exceeded 30%, the UCS values decreased regardless of the xanthan gum content. Therefore, the ideal initial moisture content corresponding to the maximum UCS for a given biopolymer content can be assumed to lie between 28% and 30%, which is 1.1 to 1.2 times the treated optimum.

The maximum UCS values for various biopolymer contents denoted by solid circles are extracted from Fig. 12 and shown in Fig. 13. Increasing the biopolymer content was effective

in enhancing the soil strength at the ideal initial moisture contents. The dosage of $m_b/m_s$ =1.0% increased the maximum UCS from 1.98 to 3.42 MPa, by 72%. As the biopolymer content further increased, the maximum UCS increased gradually and reached 4.36 MPa at $m_b/m_s$ =5.0% , by 115%.

The SEM images of the untreated soils and xanthan gum-treated soils ($m_b/m_s$=1.5% and $w$=28%) are presented in Fig. 14. It is clear that the xanthan gum-treated soils were less porous than the untreated soils on all three magnifications. This phenomenon is in line with the strength improvement. However, the SEM images for xanthan gum-treated Shanghai clay does not show inter-particle behaviour, e.g., clear biopolymer coating around the single soil particle and bridges between the detached soil particles, which is very common in the SEM images for the biopolymer-treated sands [13, 14, 18, 26]. The cementation mechanism for xanthan gum in Shanghai clay can be explained by the biopolymer-particle interaction. As xanthan gum is negatively charged, the existence of natural cations (e.g., $K^+$, $Ca^{2+}$, $Mg^{2+}$, and $Na^+$ in Fig. 3) in Shanghai clay promoted the ionic bonding between xanthan gum and Shanghai clay. In addition, the carboxylic acid (–COOH) and hydroxyl groups (–OH) of xanthan gum can easily induce hydrogen bonding [26]. The similar SEM observations for the biopolymer-treated fine soils can be found in [13, 44, 45].

### *3.4 Results of fatigue loading tests*

The fatigue life, which is the number of cycles at failure in the constant-amplitude fatigue loading tests for the samples with different xanthan gum contents, are given in Table 3. For the samples with $m_b/m_s$= 1.0% and $\sigma_m$/UCS =0.4, increasing the stress amplitude from $\sigma_a$/UCS = 0.15 to 0.3 led to a decreased fatigue life from 1,256,247 to 377,524 cycles. For the samples with $m_b/m_s$= 2.0% and $\sigma_a$/UCS= 0.15, a reduction in fatigue life from 1,945,328 to 525,271 cycles accompanied with an increment in $\sigma_m$/UCS from 0.4 to 0.6. Results from samples with $m_b/m_s$= 1.0% and $m_b/m_s$= 2.0% indicated that increasing either mean stress or stress amplitude, incurred more serious sample damage. To identify if mean stress or stress

amplitude played a more important role in the fatigue life of the xanthan gum-treated soil samples, the samples with $m_b/m_s$= 3.0% were designed to be exposed to identical $\sigma_{max}$/UCS= 0.7, but different components. It appeared that the soil was likely to have a short fatigue life with a higher ratio of $\sigma_m$/UCS for a given ratio of $\sigma_{max}$/UCS.

Furthermore, in Fig. 15, it is clear that the use of xanthan gum increased the fatigue life. For $\sigma_{max}$/UCS= 0.55, the untreated soil sample failed at 233,750 cycles, while the xanthan gum-treated soil sample with $m_b/m_s$= 1.0% failed at 1,256,247. When the $m_b/m_s$ ratio increased to 2.0%, the sample almost sustained till the end of the test. For $\sigma_{max}$/UCS= 0.70 and $\sigma_{max}$/UCS= 0.75, similar trends were observed.

For stepping-amplitude fatigue loading tests, all samples were subjected to a mean stress $\sigma_m$/UCS= 0.45 and repeated stresses increasing from $\sigma_a$/UCS= 0.05 to 0.35, at an interval of 0.1. Results of the fatigue life are given in Table 4. With the increment in $m_b/m_s$, the samples underwent more loading steps. The untreated soil sample failed under $\sigma_{max}$/UCS= 0.60 at the second step, while the sample with $m_b/m_s$= 1.0% failed under $\sigma_{max}$/UCS= 0.70, at the third step. The sample with $m_b/m_s$= 3.0%, although failed at the same loading step as the sample with $m_b/m_s$= 2.0%, had a longer fatigue life 215,869 cycles under $\sigma_{max}$/UCS=0.80 compared to 95,547 cycles for $m_b/m_s$= 2.0%.

Results from the two types of the fatigue loading tests revealed a common phenomenon. The untreated soil failed under a stress level approximately half of the UCS (e.g., $\sigma_{max}$/UCS= 0.55 to 0.6), while the xanthan gum-treated soil with $m_b/m_s$ = 3.0% sustained. With the increasing xanthan gum contents, the fatigue life increased regardless of the loading schemes.

## 4. Conclusions

The incorporation of xanthan gum in treating Shanghai clay was experimentally studied by performing standard proctor compaction tests, Atterberg limit tests, unconfined

compression, fatigue loading tests (constant-amplitude and stepping-amplitude) and microscopic analysis. Results indicated that the initial moisture content played an important role in the effectiveness of soil treatment with xanthan gum. As the initial moisture content increased from the treated optimum 26% (3% wet of the untreated optimum), the unconfined compression strength increased until a inflection point was reached, indicting an ideal initial moisture content of 1.1 to 1.2 times the treated optimum to achieve a maximum strengthening efficiency, for all five xanthan gum contents from 1.0% to 5.0%. Furthermore, either constant-amplitude or stepping-amplitude fatigue loading tests provided evidence that xanthan gum, as a eco-friendly soil strengthener, was efficient in increasing either soil bearing capacity or fatigue life, under repeated loads.

## Acknowledgments

The work described in this paper was supported by the National Natural Science Foundation of China (51608323, 51678319, 51978533), Shandong Natural Science Foundation (ZR2016EEM40) and this project has received funding from the European Union's Horizon 2020 research and innovation programme Marie Skłodowska-Curie Actions Research and Innovation Staff Exchange (RISE) under grant agreement No. 778360.

## References

[1] J.K. Mitchell, J.C. Santamarina, Biological considerations in geotechnical Engineering, J. Geotech. Geoenviron. Eng. 131 (10) (2005) 1222–1233.

[2] J.T. DeJong, K. Soga, E. Kavazanjian, S. Burns, L.A. Van PaasseN, A. Al Qabany, A. Aydilek, S.S. Bang, M. Burbank, L.F. Caslake, C.Y. Chen, X. Cheng, J. Chu, S. Ciurli, A. Esnault-Filet, S. Fauriel, N. Hamdan, T. Hata, Y. Inagaki, S. Jefferis, M. Kuo, L. Laloui, J. Larrahondo, D.A.C. Manning, B. Martinez, B.M. Montoya, D.C. Nelson, A. Palomino, P. Renforth, J.C. Santamarina, E.A. Seagren, B. Tanyu, M. Tsesarsky, T. Weaver, Biogeochemical processes and geotechnical applications: progress, opportunities and challenges, Géotechnique 63 (4) (2013) 287–301.

[3] J.T. DeJong, M.B. Fritzges, K. Nüsslein, Microbially induced cementation to control sand response to undrained shear, J. Geotech. Geoenviron. Eng. 132 (11) (2006) 1381-1392.

[4] L. Cheng, R. Cord-Ruwisch, M.A. Shahin, Cementation of sand soil by microbially induced calcite precipitation at various degrees of saturation, Can. Geotech. J. 50 (2013) 81–90.

[5] A.A. Qabany, K. Soga, Effect of chemical treatment used in MICP on engineering properties of cemented soils, Géotechnique 63 (4) (2013) 331–339.

[6] C. He, J. Chu, Undrained responses of microbially desaturated sand under monotonic loading, J. Geotech. Geoenviron. Eng. 140 (5) (2014) 04014003.

[7] D. Terzis, R. Bernier-Latmani, L. Laloui, Fabric characteristics and mechanical response of bio-improved sand to various treatment conditions, Géotechnique Lett. 6 (2016) 50–57.

[8] P. Xiao, H.L. Liu, Y. Xiao, A.W. Stuedlein, T.M. Evans, Liquefaction resistance of bio-cemented calcareous sand, Soil Dyn. Earthq. Eng. 107 (2018) 9–19.

[9] I. Chang, J. Im, G.C. Cho, Introduction of microbial biopolymers in soil treatment for future environmentally-friendly and sustainable geotechnical engineering, Sustain 8 (251) (2016a) 1–23.

[10] S.M. Viswanath, S.J. Booth, P.N. Hughes, C.E. Augarde, C. Perlot, A.W. Bruno, D. Gallipoli, Mechanical properties of biopolymer-stabilised soil-based construction materials, Géotechnique Lett. 7 (4) (2017) 309–314.

[11] N.G. Reddy, B.H. Rao, K.R. Reddy, Biopolymer amendment for mitigating dispersive characteristics of red mud waste, Géotechnique Lett. 8 (3) (2018) 201-207.

[12] C.H. Chen, L. Wu, M. Perdjon, X.Y. Hang, The drying effect on xanthan gum biopolymer treated sandy soil shear strength, Constr. Build. Mater. 197 (2019) 271–279.

[13] I. Chang, G.C. Cho, Strengthening of Korean residual soil with β-1,3/1,6-glucan biopolymer, Constr. Build. Mater. 30 (2012) 30–35.

[14] M.K. Ayeldeen, A.M. Negm, M.A. El Sawwaf, Evaluating the physical characteristics of biopolymer/soil mixtures, Arab. J. Geosci. 9 (2016) 371.

[15] H.R. Khatami, B.C. O'Kelly, Improving mechanical properties of sand using biopolymers, J. Geotech. Geoenviron. Eng. 139 (2013) 1402–1406.

[16] I. Chang, A.K. Prasidhi, J. Im, G.C, Cho. Soil strengthening using thermo-gelation biopolymers,

Constr. Build. Mater. 77 (2015b) 430–438.

[17] I. Chang, J. Im, G.C. Cho, Geotechnical engineering behaviors of gellan gum treated sand, Can. Geotech. J. 53 (2016b) 1658-1670.

[18] I. Chang, J. Im, S.W. Lee, G.C. Cho, Strength durability of gellan gum biopolymer-treated Korean sand with cyclic wetting and drying, Constr. Build. Mater. 143 (2017) 210–221.

[19] I. Chang, G.C. Cho, Shear strength behavior and parameters of microbial gellan gum-treated soils: from sand to clay, Acta. Geotech. 14 (2019) 361–375.

[20] R. Aguilar, J. Nakamatsu, E. Ramírez, M. Elgegren, J. Ayarza, S. Kim, M.A. Pando, L. Ortega-San-Martin, The potential use of chitosan as a biopolymer additive for enhanced mechanical properties and water resistance of earthen construction, Constr. Build. Mater. 114 (2016) 625–637.

[21] N. Hataf, P. Ghadir, N. Ranjbar, Investigation of soil stabilization using chitosan biopolymer, J. Clean Prod. 170 (2018) 1493–1500.

[22] J. Nakamatsu , S. Kim, J. Ayarza, E. Ramírez, M. Elgegren, R. Aguilar, Eco-friendly modification of earthen construction with carrageenan: Water durability and mechanical assessment, Constr. Build. Mater. 139 (2017) 193–202.

[23] H. Fatehi, S.M. Abtahi, H. Hashemolhosseini, S.M. Hejazi, A novel study on using protein-based biopolymers in soil strengthening, Constr. Build. Mater. 167 (2018) 813–821.

[24] I. Chang, J. Im, M.K. Chung, G.C. Cho, Bovine casein as a new soil strengthening binder from diary wastes, Constr. Build. Mater. 160 (2018a) 1–9.

[25] P. Ghadir, N. Ranjbar, Clayey soil stabilization using geopolymer and Portland cement, Constr. Build. Mater. 188 (2018) 361-371.

[26] I. Chang, J. Im, A.K. Prasidhi, G.C. Cho, Effects of xanthan gum biopolymer on soil strengthening, Constr. Build. Mater. 74 (2015a) 65–72.

[27] N. Latifi, S. Horpibulsuk, C.L. Meehan, M.Z.A. Majid, A.S.A. Rashid, Xanthan gum biopolymer: an eco-friendly additive for stabilization of tropical organic peat, Environ. Earth. Sci. 75 (2016) 825.

[28] G.C. Barrére, C.E. Barber, M.J. Daniels, Molecular cloning of genes involved in the production of the extracellular polysaccharide xanthan by Xanthomonas campestris pv. Campestris, Int. J. Biol.

Macromol. 8 (1986) 372–374.

[29] S. Rosalam, R. England, Review of xanthan gum production from unmodified starches by xanthomonas comprestris sp, Enzyme Microb. Technol. 39 (2) (2006) 197–207.

[30] C. Lam, S.A. Jefferis, The use of polymer solutions for deep excavations: lessons from Far Eastern experience. HKIE Transactions 21 (4) (2014) 262-271.

[31] C. Lam, S.A. Jefferis, Polymer Support Fluids in Civil Engineering, ICE, 2017.

[32] R. Guerrero-Lemus, J.M. Martinez-Duart, Renewable energies and $CO_2$: Cost Analysis, Environmental Impacts and Technological Trends, 2012 edition, Springer London, UK, 2013.

[33] H.B. Seed, C.K. Chan, Clay strength under earthquake loading conditions, J. Soil Mech. Found. Div. 92 (2) (1966) 53–78.

[34] J.P. Carter, J.R. Booker, C.P. Wroth, A critical state soil model for cyclic loading, Soil mechanics—Transient and cyclic loading (1982) 219–252.

[35] J.C. Chai, N. Miura, Traffic-load-induced permanent deformation of road on soft subsoil, J. Geotech. Geoenviron. Eng. 128 (11) (2002) 907–916.

[36] X.Y. Geng, C. Xu, Y. Cai, Non-linear consolidation analysis of soil with variable compressibility and permeability under cyclic loadings, Int. J. Numer. Anal. Met. 30 (8) (2006) 803–821.

[37] K.H. Andersen, Bearing capacity under cyclic loading—offshore, along the coast, and on land, Can. Geotech. J. 46 (5) (2007) 513–535.

[38] J. Ni, I. Indraratna, X.Y. Geng, J.P. Carter, Y.L. Chen, Model of soft soils under cyclic loading, Int. J. Geomech. 15 (4) (2015) 04014067 (10 pp.).

[39] Y.L. Chen, J. Ni, P. Zheng, R. Azzam, Y.C. Zhou, W. Shao, Experimental research on the behaviour of high frequency fatigue in concrete, Eng. Fail Anal. 18 (2011) 1848–1857.

[40] Y.L. Chen, J. Ni, W. Shao, Y.C. Zhou, A. Javadi, R. Azzam, Coalescence of fractures under uni-axial compression and fatigue loading, Rock Mech. Rock. Eng. 45 (2012a) 241–249.

[41] Y.L. Chen, J. Ni, W. Shao, R. Azzam, Experimental study on the influence of temperature on the mechanical properties of granite under uni-axial compression and fatigue loading, Int. J. Rock Mech. Min. 56 (2012b) 62–66.

[42] B.M. Lekha, G. Sarang, A.U.R. Shankar, Effect of electrolyte lignin and fly ash in stabilizing

black cotton soil, Transp. Infrastruct. Geotech. 2 (2015) 87–101.

[43] I. Chang, Y.M. Kwon, J. Im, G.C. Cho, Soil consistency and interparticle characteristics of xanthan gum biopolymer – containing soils with pore-fluid variation, Can. Geotech. J. 56 (8) (2019) 1206–1213.

[44] A. Soldo, M. Miletić, M.L. Auad, Biopolymers as a sustainable solution for the enhancement of soil mechanical properties, Sci. Rep-Uk. 10 (1) (2020) 213-267.

[45] A.S.A. Rashid, S. Tabatabaei, S. Horpibulsuk, N.Z. Mohd Yunus, W.H.W. Hassan, Shear Strength Improvement of Lateritic Soil Stabilized by Biopolymer Based Stabilizer, Geotechnical and Geological Engineering 37 (6) (2019) 5533-5541.

# Performance of soils enhanced with eco-friendly biopolymers in unconfined compression strength tests and fatigue loading tests

**Jing Ni[a], Shan-Shan Li[a], Lei Ma[a], Xue-Yu Geng[b,*]**

[a]*Department of Civil Engineering, University of Shanghai for Science and Technology, 200093 Shanghai, P.R. China.*

[b]*School of Engineering, University of Warwick, Coventry, CV4 7AL, UK (*corresponding author)*

***Corresponding author**: Xue-Yu Geng (Email: xueyu.geng@warwick.ac.uk)

**Abstract** Recently, biopolymers have emerged in soil stabilisation. The efficiency of biopolymers in ground improvement is mainly dependent on biopolymer types, soil types, biopolymer contents, curing periods, thermal treatment and mixing methods. However, the effect of the initial moisture content during sample preparation stages, on the mechanical behaviours of biopolymer-treated soils, has not been fully understood. The first part of this study probed the role of initial moisture content, in treating Shanghai clay with the xanthan gum by performing standard proctor compaction tests, Atterberg limit tests, unconfined compression strength (UCS) tests and microstructural analysis, while the second part contributed to capture the fatigue behaviours of the samples treated with an ideal moisture content by performing constant-amplitude and stepping-amplitude fatigue loading tests. Our results showed that the improvement appeared to occur from an average optimum moisture content for the treated soils (treated optimum), which was 3% wet of the untreated optimum. As the initial moisture content increased, the UCS values were elevated. However, there existed an ideal initial moisture content leading to the maximum strengthening efficiency. For xanthan gum content (i.e., the mass of xanthan gum with respect to the mass of dry soil) ranging from 1.0% to 5.0%, this ideal value was between 1.1 and 1.2 times the treated optimum. Our results also indicated that xanthan gum, as a biopolymer soil strengthener, was efficient in increasing either fatigue life or bearing capacity, under repeated loading for xanthan gum-soil matrices, when compared to untreated soils. While the untreated soils failed at the stress level of only half the UCS, the xanthan gum-treated soils with a 3.0% xanthan gum content sustained at the end of the tests. These data imply the potential use of xanthan gum in soil stabilisation, under repeated loads.

**Keywords** Xanthan gum, Initial moisture content, Unconfined compression strength, Repeated loads, Ground improvement

## 1. Introduction

During the past two decades, the application of biological processes to soil stabilisation has emerged in geotechnical engineering [1, 2]. Bio-mineralisation, which leads to mineral precipitation using the bio-technological mediation route, has been extensively investigated as a bio-treatment for soils [3-8]. More recently, the direct use of biogenic excrement (i.e., biopolymers) as a ground improvement method has gained increased academic interest, as biopolymers are abundant in nature and are considered eco-friendly materials for soil treatment [9], and on the other hand able to improve soil strength, even under a very low biopolymer-to-soil ratio (e.g., 0.5%) [10-12].

As a commonly applied contemporary biopolymer type in various practices, polysaccharides have been evaluated for their capacity to treat soils. Beta-glucan ($\beta$-1, 3/1, 6-glucan) and guar gum have been found operational and effective in enhancing the mechanical strength of soils [13, 14]. Gellan gum and agar gum have similar properties, including thermos-gelation and significant efficiency in strengthening soils [15-19]. The application of carrageenan and chitosan as additives to earthen constructions contributes positively on water durability [20-22]. In addition to polysaccharides, the incorporation of protein-based biopolymers (e.g., casein and sodium caseinate salt) to improve the mechanical properties and durability of natural soils has also been reported [23, 24].

Throughout the literature, it has been recognized that the efficiency of biopolymers in ground improvement is mainly dependent on biopolymer types, soil types, biopolymer contents, curing periods, thermal treatment and mixing methods. The effect of the moisture content on the performance of biopolymer-treated soils, however, has not been fully understood. Some researchers have revealed that the biopolymer-treated soils [12, 24], like other geopolymer-treated soils [25], appear to have a higher mechanical strength with a lower value of moisture content. During the sample preparation stage, a reduction in the initial moisture content may lead to an increased strength [19], which is illustrated in Fig. 1 (Zone

*A*). However, the strength is unlikely to continue increasing when the initial moisture content decreases (Fig. 1, Zone *C*), as too little water results in a poorly dissolved biopolymer solution, which could adversely affect the workability of the biopolymer-soil matrix and its consequent mechanical strength [26]. As a result, there might exist an ideal initial moisture content ($w_I$) leading to the highest strength as illustrated in Fig. 1, i.e., inflection point from Zone *B* to Zone *A*. Therefore, the initial moisture content appears to play an important role in the efficiency of soil treatment. Up to now, little research has been performed in this area. Usually, the initial moisture content has been set as a fixed value, e.g., liquid limit [13, 16, 26], optimum moisture content [21, 23], and natural moisture content [27].

In this study, the effect of the initial moisture content on the efficiency of soil treatment will be probed by an experimental study on the xanthan gum-treated Shanghai clay. Xanthan gum has been extensively researched in the soil treatment due to its unique functional properties. It has excellent cold water dissolving capacity, pH stability, storage stability, ionic salt compatibility, and pseudo-plastic flow characteristics [28, 29]. For geotechnical engineering, xanthan gum has been used as polymer support fluids to stabilize deep excavations [30, 31]. Recent studies have reported that xanthan gum, providing bonds between soil particles, has the potential to act as a soil strengthener [12, 14, 26, 27]. In addition, the presence of xanthan gum in soils reduces the hydraulic conductivity due to the "clogging effect", and enables hydrogen bonds to enhance the strength and corrosion resistance of sands [14, 26, 27].

On the other hand, xanthan gum are available at reasonable prices. In general, the market prices of biopolymers are more expensive than conventional soil stabilizers and inorganic binders (e.g., geopolymers). However, taken into account the global greenhouse gas reduction efforts (e.g., carbon emission trading), biopolymers will become remarkably competitive in soil treatment, e.g., for a unit amount (1 ton) of soil treatment, 0.5% xanthan gum is only 3.6% more expensive than 10% cement [9, 32]. In addition, the biopolymers have higher production

costs due to their widespread use in the fields of food production, agriculture, and medical treatment. For geotechnical applications, it is expected that the price of biopolymers will be greatly reduced due to the unnecessary edible standards [9, 14].

To the authors' knowledge, limited research has accessed the fatigue behaviours of the xanthan gum-treated soils. Soils subjected to repeated loads can fail under a stress level consisting only a fraction of a static strength [33-41]. Therefore, a lack of understanding of the mechanical behaviours of the biopolymer-treated soils under fatigue loading will restrict the evaluation of their long-term resilience and practical engineering performances (e.g., highway pavements, railway tracks, and airport runways). Given this background, this study involved investigating the performances of xanthan gum-treated soils from two aspects, i.e., the ideal treatment condition (e.g., ideal initial moisture content) to achieve the maximum strengthening effect and fatigue behaviours under the ideal treatment condition. Standard proctor compaction tests and Atterberg limit tests were also performed along with the SEM images to better understand the underlying strengthening mechanisms.

## 2. Materials and Methods

### *2.1. Shanghai clay*

Shanghai lies in the Yangtze River delta alluvial plain in China. For this study, natural soils were sampled from a construction site of Metro Line 15 in the northwest Shanghai, at a depth of 8.9 m. Table 1 shows some of the basic engineering properties for Shanghai clay, e.g., optimum moisture content (OMC) and maximum dry density ($\rho_{dmax}$), and gravimetric-volumetric parameters.

Particle size distribution analysis was performed on the soil using a Mastersizer 3000 particle size analyser (Malvern, UK), which caters for the particles in the range of 10 nm to 3.5 mm. As shown in Fig. 2, the natural soil had 33.41% by weight sand content, 54.86% silt

content, and 11.73% clay content based on the soil particle size ranges as recommended in ASTM D422. The Atterberg limits, i.e., the liquid and plastic limits of the natural soil, were found to be $w_L$=37.9% and $w_P$=22%, respectively. The corresponding plastic index was $I_P$=15.9%. Combined with the particle size distribution curve and Atterberg limits, the natural soil was therefore classified as sand lean clay, as per ASTM D2487.

An X-ray fluorescence (XRF) test on the soil was performed using a portable QUANTAX energy-dispersive X-ray microanalysis (EDX) spectrometer (Brucker, Germany), equipped with a 2.5 kg probe, 50 W pulse processor and Esprit analysis software. The XRF spectrum (Fig. 3) indicated that the most abundant elements were Si, C, O, Al, K, Mg, Na, and Fe.

Mineralogical analysis of the natural soil was conducted using the X-ray powder diffraction test (XRPD), using a D8 ADVANCE diffractometer (Brucker, Germany). Data was automatically collected for phase angles ($2\theta$), ranging between 5º and 90º, at 0.02º intervals. Identification of the crystalline phases was carried out using JADE software. XRPD patterns are shown in Fig. 4, including main peak identification, $SiO_2$.

### *2.2. Xanthan gum*

Xanthan gum is a polysaccharide formed by the fermentation of sugar (e.g., glucose or sucrose) by the bacterium *Xanthomonas campestris.* It was chosen to treat Shanghai clay for its unique functional properties and reasonable prices as previously demonstrated. The xanthan gum powder for this study was manufactured by Shandong Fengtai Biological Technology Co., Ltd.

### *2.3. Sample fabrication*

Sample preparation for both unconfined compression strength tests and fatigue loading tests followed the same procedures. The Shanghai clay was oven dried (105 ºC) for 24 hours,

broken down carefully with rubber hammers, and sieved using a 2 mm sieve to obtain a base soil. The base soil was thoroughly mixed with xanthan gum, before distilled water was added. To increase the solubility, the distilled water was heated to 80 ºC [26]. A metal trowel was used for mixing manually for about five minutes until a homogeneous xanthan gum-soil mixture was obtained. The mixture was then placed inside a cylindrical mould with an inner diameter of 39.1 mm and a height of 80 mm in three layers. For each layer, 25 blows were applied through a rammer (305.5 g) dropping from a height of 247 mm. The compacted samples were extruded after compaction, and cured in a controlled environment at 60% relative humidity and 20 ºC for 28 days.

### 2.4 *Experimental programme*

The experimental program involved exploring the influence of using xanthan gum on the behaviours of Shanghai clay from five aspects: (1) compaction properties; (2) Atterberg limits; (3) microscopic structures; (4) mechanical properties under unconfined compression and (5) fatigue loading. The following subsections present the test procedures for each component of the experimental programme. Each test was replicated at least three times to achieve a reliable average.

#### *2.4.1* Standard proctor compaction tests

The standard proctor compaction tests were conducted in accordance with ASTM D698 to determine the maximum dry density and its corresponding optimum moisture content for xanthan gum-treated soil samples. Five xanthan gum contents (the mass of xanthan gum with respect to the mass of dry soil), e.g., $m_b/m_s$=1.0%, 2.0%, 3.0%, 4.0%, and 5.0% (Table 2), were used to investigate the variation of compaction properties with the increasing xanthan gum content.

#### *2.4.2* Atterberg limit tests

The Atterberg limits ($w_P$ and $w_L$) of the soils treated with five xanthan gum contents (Table 2) were determined by Liquid-Plastic Limit Combined Test (GB/T 50123-2019, Part 9) by using a cone with a mass of 76 g and a tip angle of 30°. The penetration depth of the cone into the sample (55 mm diameter and 40 mm height) was measured 5 s after the cone had been released. For each biopolymer content, the test was repeated on five samples with an increased moisture content. The water contents corresponding to 17 mm and 2 mm determined with the aid of a linear fitting curve in the semi-log plane of cone penetration-moisture content were regarded as liquid limit and plastic limit, respectively.

### *2.4.3.* Unconfined compression strength tests

The effectiveness of incorporating xanthan gum in improving the soil strength at different initial moisture contents was investigated by the unconfined compression strength tests, which were conducted under the strain-controlled condition at a loading rate of 1.5%/min in accordance with ASTM D2166. The xanthan gum contents used were the same as those adopted for the standard proctor compaction and Atterberg limit tests. For each biopolymer content, five initial moisture contents were employed (Table 2). As suggested by Fatehi et al. [23] and Hataf et al. [21], the optimum moisture content of the untreated soil ($w$=23%) (hereafter referred as untreated optimum) was adopted as the minimum initial moisture content. The xanthan gum-treated soil samples with $w$=23% had a lot of voids on the sample surfaces, indicating an unthorough mixing due to the poor workability of the xanthan gum-soil mixture. Then 3% wet of the untreated optimum was selected based on the results of the standard proctor compaction tests (section 2.4.1), which indicated that the mean value of the optimum moisture contents of the treated soils (hereafter referred as treated optimum) with various xanthan gum contents was $w$=26%. Afterwards, the initial moisture content was increased at an interval of 2%. With the increment in the amount of water for sample mixing, the workability of the xanthan gum-soil mixture was improved. However, as the initial moisture content reached 34%, the compacted samples were visually deformed after they

were extruded from the cylindrical mould. Therefore, $w$=32% was adopted as the maximum initial moisture content. The untreated soil sample, prepared with the optimum moisture content $w$=23%, served as a control sample.

### *2.4.4. Fatigue loading tests*

Apart from the unconfined compression strength tests, fatigue loading tests were performed on the xanthan gum-treated soil samples as well. These samples used $w$=30%, and $m_b/m_s$ = 1.0%, 2.0%, and 3.0%. They were cured under the controlled conditions for 28 days before being exposed to the fatigue loading tests. The ZWICK-100HFP5100 test apparatus (ZwickRoell, Germany) was employed to apply fatigue loads. For detailed descriptions see Chen et al. [42-44]. The test procedure started with the mounting of cylindrical samples on the loading frame and bringing the load cell into contact with the sample surface. Through the user-friendly visualisation window, the mean stress, stress amplitude, and maximum loading cycles were fed into the load application device. The loading system was switched on at the same time as the automatic data acquisition system, and fatigue loading was initiated. The process continued until failure of the sample, or the maximum loading cycle was reached.

In this study, the fatigue loading tests involved two strategies: constant-amplitude and stepping-amplitude. In the constant-amplitude tests, the mean stress ($\sigma_m$) and stress amplitude ($\sigma_a$) for each sample remained constant during the loading process. In the stepping-amplitude tests, the mean stress remained constant, but the stress amplitude increased stepwise. Details of the two components of fatigue loading test are described as follows.

The loading schemes for the constant-amplitude and stepping-amplitude fatigue loading tests are shown in Fig. 5. The test input parameters included the mean stress($\sigma_m$) and stress amplitude ($\sigma_a$). The corresponding maximum stress ($\sigma_{max}=\sigma_m+\sigma_a$) and the minimum stress ($\sigma_{min}=\sigma_m-\sigma_a$) were calculated. The effects of $\sigma_m$, $\sigma_a$ and their combination on fatigue life were investigated. The test matrix of constant-amplitude fatigue loading tests is given in Table 3.

The maximum stress were from 1/2 to 3/4 fractions of UCS values referring to Lekha et al. [45], corresponding to medium to high stress levels. The UCS for each treatment condition was used as a basis for the calculation of fatigue stresses (e.g., $\sigma_m$, $\sigma_a$, $\sigma_{max}$, and $\sigma_{min}$). The maximum number of loading cycles for each test was set as 2,000,000. The loading frequency was set as a resonant frequency between the sample and the apparatus, which was about 40 to 45 Hz, rather than a fixed value.

For the stepping-amplitude fatigue loading tests, the mean stress ($\sigma_m$) for each sample was constant, while the stress amplitude ($\sigma_a$) increased step by step, at a constant interval. For each loading step, 500,000 cycles of fatigue loading were applied. The fatigue loading tests started from the first step and stopped until either the designed number of cycles was reached, or the sample failed. The test matrix of the stepping-amplitude fatigue loading tests are given in Table 4.

#### *2.4.5. Microscopic structures*

Scanning electrons microscope (SEM) and field emission scanning electron microscope (FESEM) have been used to explore the microstructural characteristics of biopolymer-treated soils, including shapes, sizes, and aggregation of soil particles [19, 23, 27]. In this study, SEM images were taken for both untreated soils and xanthan gum-treated soils ($m_b/m_s$=1.5% and $w$=28%). Microstructural analysis was conducted to better understand the connection between xanthan gum and Shanghai clay, and furthermore the underlying mechanisms of soil stabilization.

## *3. Results and discussion*

### *3.1 Effect of biopolymer contents on compaction characteristics*

The introduction of xanthan gum altered the compaction characteristics of Shanghai clay. The optimum moisture content was observed to increase from 23% to 26.7%. and the

maximum dry density had a descending trend falling from 1.59 g/cm$^3$ to 1.51 g/cm$^3$, as the xanthan gum content increased from $m_b/m_s$= 0.0% to 5.0% (Fig. 6). Ayeldeen et al. [14] reported that this alteration may depend on both the biopolymer characteristics (e.g., chemical properties and solution viscosities) and soil fine-grained content. In the current study, xanthan gum molecules contain a large number of hydrophilic groups (e.g., -OH and -COOH) and therefore have a large capacity to attract water molecules or dissolve in water, and retain water. As a result, elevating the xanthan gum content increased the amount of absorbed water, and therefore increased the optimum moisture content and decreased the maximum dry density.

### *3.2 Effect of biopolymer contents on Atterberg limits*

The liquid limit increased obviously from 37.9% to 44.9% as the $m_b/m_s$ ratio increased from 0.0% to 1.0%, and then slightly increased with the increasing xanthan gum content, to a maximum value of 51.1% at $m_b/m_s$= 5.0%, as shown in Fig. 7. The increasing trend of liquid limit of xanthan gum-soil matrix was also observed by Chang et al. [46]. The mechanism responsible for this phenomenon is similar to that works in compacting xanthan gum-treated soil (e.g., hydrophilic properties and water retention capacity). Treated samples with a higher xanthan gum content had a higher content of hydrophilic xanthan gum hydrogel, leading to a higher liquid limit. Simultaneously, the plastic limit increased gradually from 22% to 25.7% as the xanthan gum content increased from 0.0% to 5.0%.

### *3.3. Results of unconfined compression strength tests*

#### *3.3.1 Effect of initial moisture content on Stress-strain behaviour*

The typical stress-strain curves for five xanthan gum contents at an initial moisture content $w$=30% are shown in Fig. 8. The trends of axial stress versus axial strain of xanthan gum-treated soil samples differed gradually from that of the untreated soil sample ($m_b/m_s$=

0.0%) with the increasing $m_b/m_s$ ratio, indicating that adding xanthan gum to soils provided strengthening effects. On the other hand, the xanthan gum-treated soil samples were more deformable, i.e., the peak axial strain corresponding to the peak axial stress increased from 1.67% to 5.12% as the xanthan gum content increased from 0.0% to 5.0%.

When the initial moisture content was reduced to the treated optimum $w$=26%, the xanthan gum-treated soils also had improved stress-strain behaviours (Fig. 9), however, not as prominent as those for 30% initial moisture content. This implies that using the treated optimum as an initial moisture content did not necessarily lead to the best strengthening effect. This may be due to the undesirable workability caused by insufficient water for xanthan gum-soil matrix mixing. As described in the previous section 3.2, the plastic limit of the xanthan gum-soil matrix increased as a result of increasing the xanthan gum content. Therefore, the initial moisture content of 26% was slightly larger than the plastic limit of the soil samples after they had been treated with xanthan gum at $m_b/m_s$ ratio ranging from 1.0 to 5.0% ($w_p$= 23.5 to 25.7%).

The moisture-dependent stress-strain behaviour is further illustrated in Fig. 10. For a given value of $m_b/m_s$= 1.0%, the efficiency of xanthan gum in improving the soil mechanical behaviour was intimately related to the initial moisture content. Four of the five stress-strain curves for xanthan gum-treated soils lie above the untreated soil, indicating the strengthening effect can only be obtained for a moisture content larger than 26% (treated optimum). The treated samples prepared with the untreated optimum (23%) seemed not to differ from the untreated sample. The similar phenomenon was also observed for $m_b/m_s$ = 2.0% prepared with the untreated optimum. This could be explainable that $w$=23% was even smaller than the plastic limit of the xanthan gum-treated soils, which resulted in an unthorough mixing and prevented the xanthan gum to be an efficient binder. In addition, the strength was observed to reach a maximum value of 3.47 MPa at the initial water content $w$=30%, where either a smaller value $w$=28% or a larger value $w$=32% resulted in a reduced peak axial stress. This

phenomenon indicates that there exists an ideal initial moisture content that can lead to a maximum strengthening effect.

### *3.3.2 Effect of initial moisture content on UCS*

The variation of the unconfined compression strength (UCS) defined as the peak axial stress, with an increasing initial moisture content for untreated soils are shown in Fig. 11. The UCS underwent an increase and then a decrease as the initial moisture content increased from 17% to 30% with a peak value of 1.98 MPa at the optimum moisture content $w$=23%.

Figure 12 shows the trends of UCS with an increasing moisture content for five biopolymer contents. For a given value of $m_b/m_s$=1.0%, the UCS initially increased from 2.67 MPa to a peak value of 3.42 MPa as the initial moisture content increased from 26% to 30%. Afterwards, additional amount of water led to a reduced UCS value of 2.98 MPa. This trend retained when $m_b/m_s$ =1.0% was replaced with $m_b/m_s$ =4.0% and 5.0%. For $m_b/m_s$= 2.0% and 3.0%, the UCS values also underwent an increment and a decrement with the increasing moisture content, but the peak value of UCS was observed at $w$=28%.

The overall trend of UCS indicate that xanthan gum-treated soil samples with all five biopolymer contents grained strength as the moisture content increased from 26% to 28%. Further elevating the moisture content from 28% to 30% led to an increased UCS for $m_b/m_s$ =1.0%, 4.0% and 5.0% and a decreased UCS for $m_b/m_s$ =2.0% and 3.0%. Afterwards, as the moisture content exceeded 30%, the UCS values decreased regardless of the xanthan gum content. Therefore, the ideal initial moisture content corresponding to the maximum UCS for a given biopolymer content can be assumed to lie between 28% and 30%, which is 1.1 to 1.2 times the treated optimum.

The maximum UCS values for various biopolymer contents denoted by solid circles are extracted from Fig. 12 and shown in Fig. 13. Increasing the biopolymer content was effective

in enhancing the soil strength at the ideal initial moisture contents. The dosage of $m_b/m_s$ =1.0% increased the maximum UCS from 1.98 to 3.42 MPa, by 72%. As the biopolymer content further increased, the maximum UCS increased gradually and reached 4.36 MPa at $m_b/m_s$ =5.0% , by 115%.

The SEM images of the untreated soils and xanthan gum-treated soils ($m_b/m_s$=1.5% and $w$=28%) are presented in Fig. 14. It is clear that the xanthan gum-treated soils were less porous than the untreated soils on all three magnifications. This phenomenon is in line with the strength improvement. However, the SEM images for xanthan gum-treated Shanghai clay does not show inter-particle behaviour, e.g., clear biopolymer coating around the single soil particle and bridges between the detached soil particles, which is very common in the SEM images for the biopolymer-treated sands [13, 14, 18, 26]. The cementation mechanism for xanthan gum in Shanghai clay can be explained by the biopolymer-particle interaction. As xanthan gum is negatively charged, the existence of natural cations (e.g., $K^+$, $Ca^{2+}$, $Mg^{2+}$, and $Na^+$ in Fig. 3) in Shanghai clay promoted the ionic bonding between xanthan gum and Shanghai clay. In addition, the carboxylic acid (–COOH) and hydroxyl groups (–OH) of xanthan gum can easily induce hydrogen bonding [26]. The similar SEM observations for the biopolymer-treated fine soils can be found in [13, 47, 48].

### *3.4 Results of fatigue loading tests*

The fatigue life, which is the number of cycles at failure in the constant-amplitude fatigue loading tests for the samples with different xanthan gum contents, are given in Table 3. For the samples with $m_b/m_s$= 1.0% and $\sigma_m$/UCS =0.4, increasing the stress amplitude from $\sigma_a$/UCS = 0.15 to 0.3 led to a decreased fatigue life from 1,256,247 to 377,524 cycles. For the samples with $m_b/m_s$= 2.0% and $\sigma_a$/UCS= 0.15, a reduction in fatigue life from 1,945,328 to 525,271 cycles accompanied with an increment in $\sigma_m$/UCS from 0.4 to 0.6. Results from samples with $m_b/m_s$= 1.0% and $m_b/m_s$= 2.0% indicated that increasing either mean stress or stress amplitude, incurred more serious sample damage. To identify if mean stress or stress

amplitude played a more important role in the fatigue life of the xanthan gum-treated soil samples, the samples with $m_b/m_s$= 3.0% were designed to be exposed to identical $\sigma_{max}$/UCS= 0.7, but different components. It appeared that the soil was likely to have a short fatigue life with a higher ratio of $\sigma_m$/UCS for a given ratio of $\sigma_{max}$/UCS.

Furthermore, in Fig. 15, it is clear that the use of xanthan gum increased the fatigue life. For $\sigma_{max}$/UCS= 0.55, the untreated soil sample failed at 233,750 cycles, while the xanthan gum-treated soil sample with $m_b/m_s$= 1.0% failed at 1,256,247. When the $m_b/m_s$ ratio increased to 2.0%, the sample almost sustained till the end of the test. For $\sigma_{max}$/UCS= 0.70 and $\sigma_{max}$/UCS= 0.75, similar trends were observed.

For stepping-amplitude fatigue loading tests, all samples were subjected to a mean stress $\sigma_m$/UCS= 0.45 and repeated stresses increasing from $\sigma_a$/UCS= 0.05 to 0.35, at an interval of 0.1. Results of the fatigue life are given in Table 4. With the increment in $m_b/m_s$, the samples underwent more loading steps. The untreated soil sample failed under $\sigma_{max}$/UCS= 0.60 at the second step, while the sample with $m_b/m_s$= 1.0% failed under $\sigma_{max}$/UCS= 0.70, at the third step. The sample with $m_b/m_s$= 3.0%, although failed at the same loading step as the sample with $m_b/m_s$= 2.0%, had a longer fatigue life 215,869 cycles under $\sigma_{max}$/UCS= 0.80 compared to 95,547 cycles for $m_b/m_s$= 2.0%.

Results from the two types of the fatigue loading tests revealed a common phenomenon. The untreated soil failed under a stress level approximately half of the UCS (e.g., $\sigma_{max}$/UCS= 0.55 to 0.6), while the xanthan gum-treated soil with $m_b/m_s$= 3.0% sustained. With the increasing xanthan gum contents, the fatigue life increased regardless of the loading schemes.

### *3.5 Possible implementations of xanthan gum in geotechnical engineering practices*

Although this is a laboratory study, how soft clays can be treated with xanthan gum in practice is briefly discussed as follows.

The incorporation of xanthan gum into soils on site can be conducted through deep mixing, spraying, grouting, high-pressure injection, and etc. [9, 31, 49]. Given the high viscosity of xanthan gum solution that is prone to block the voids in soils for further solution penetration, deep mixing might be recommended. In the existing laboratory research, biopolymers have been introduced into the soil in power or solution form (i.e., dry mixing or wet mixing). According to Arab et al. [50], wet mixing method is more effective in treating different cohesive soils with sodium alginate. Ayeldeen et al. [14] observed that the efficiency of xanthan gum or guar gum through wet mixing in reducing collapsibility was about 2-3 times more than dry mixing, while Chang et al. [26] reported that dry mixing is more effective than wet mixing by providing a well-distributed xanthan matrix in soil given that the amount of mixing water is sufficient for xanthan gum dissolution. As for practical applications, dry mixing is considered as an appropriate method [51]. Therefore, the choice of mixing method in practice may need to be determined according to the solubility, the addition amount and types of biopolymers, and soil types. Furthermore, various factors such as workability, construction cost, relevant machinery, and environmental issue need to be assessed for practical and economic application on site.

## 4. Conclusions

The incorporation of xanthan gum in treating Shanghai clay was experimentally studied by performing standard proctor compaction tests, Atterberg limit tests, unconfined compression, fatigue loading tests (constant-amplitude and stepping-amplitude) and microscopic analysis. Results indicated that the initial moisture content played an important role in the effectiveness of soil treatment with xanthan gum. As the initial moisture content increased from the treated optimum 26% (3% wet of the untreated optimum), the unconfined compression strength increased until a inflection point was reached, indicting an ideal initial moisture content of 1.1 to 1.2 times the treated optimum to achieve a maximum strengthening efficiency, for all five xanthan gum contents from 1.0% to 5.0%. Furthermore, either

constant-amplitude or stepping-amplitude fatigue loading tests provided evidence that xanthan gum, as a eco-friendly soil strengthener, was efficient in increasing either soil bearing capacity or fatigue life, under repeated loads.

## Acknowledgments

The work described in this paper was supported by the National Natural Science Foundation of China (51608323, 51678319, 51978533). In addition, this project has received funding from the European Union's Horizon 2020 Framework programme Marie Skłodowska-Curie Individual Fellowships under grant agreement No. 897701 and Marie Skłodowska-Curie Actions Research and Innovation Staff Exchange (RISE) under grant agreement No. 778360.

## References

[1] J.K. Mitchell, J.C. Santamarina, Biological considerations in geotechnical Engineering, J. Geotech. Geoenviron. Eng. 131 (10) (2005) 1222–1233.

[2] J.T. DeJong, K. Soga, E. Kavazanjian, S. Burns, L.A. Van PaasseN, A. Al Qabany, A. Aydilek, S.S. Bang, M. Burbank, L.F. Caslake, C.Y. Chen, X. Cheng, J. Chu, S. Ciurli, A. Esnault-Filet, S. Fauriel, N. Hamdan, T. Hata, Y. Inagaki, S. Jefferis, M. Kuo, L. Laloui, J. Larrahondo, D.A.C. Manning, B. Martinez, B.M. Montoya, D.C. Nelson, A. Palomino, P. Renforth, J.C. Santamarina, E.A. Seagren, B. Tanyu, M. Tsesarsky, T. Weaver, Biogeochemical processes and geotechnical applications: progress, opportunities and challenges, Géotechnique 63 (4) (2013) 287–301.

[3] J.T. DeJong, M.B. Fritzges, K. Nüsslein, Microbially induced cementation to control sand response to undrained shear, J. Geotech. Geoenviron. Eng. 132 (11) (2006) 1381-1392.

[4] L. Cheng, R. Cord-Ruwisch, M.A. Shahin, Cementation of sand soil by microbially induced calcite precipitation at various degrees of saturation, Can. Geotech. J. 50 (2013) 81–90.

[5] A.A. Qabany, K. Soga, Effect of chemical treatment used in MICP on engineering properties of cemented soils, Géotechnique 63 (4) (2013) 331–339.

[6] C. He, J. Chu, Undrained responses of microbially desaturated sand under monotonic loading, J. Geotech. Geoenviron. Eng. 140 (5) (2014) 04014003.

[7] D. Terzis, R. Bernier-Latmani, L. Laloui, Fabric characteristics and mechanical response of bio-improved sand to various treatment conditions, Géotechnique Lett. 6 (2016) 50–57.

[8] P. Xiao, H.L. Liu, Y. Xiao, A.W. Stuedlein, T.M. Evans, Liquefaction resistance of bio-cemented calcareous sand, Soil Dyn. Earthq. Eng. 107 (2018) 9–19.

[9] I. Chang, J. Im, G.C. Cho, Introduction of microbial biopolymers in soil treatment for future environmentally-friendly and sustainable geotechnical engineering, Sustainability 8 (3) (2016) 251.

[10] S.M. Viswanath, S.J. Booth, P.N. Hughes, C.E. Augarde, C. Perlot, A.W. Bruno, D. Gallipoli, Mechanical properties of biopolymer-stabilised soil-based construction materials, Géotechnique Lett. 7 (4) (2017) 309–314.

[11] N.G. Reddy, B.H. Rao, K.R. Reddy, Biopolymer amendment for mitigating dispersive characteristics of red mud waste, Géotechnique Lett. 8 (3) (2018) 201-207.

[12] C. Chen, L. Wu, M. Perdjon, X. Huang, Y. Peng, The drying effect on xanthan gum biopolymer treated sandy soil shear strength, Constr. Build. Mater. 197 (2019) 271–279.

[13] I. Chang, G.C. Cho, Strengthening of Korean residual soil with $\beta$-1, 3/1, 6-glucan biopolymer, Constr. Build. Mater. 30 (2012) 30–35.

[14] M.K. Ayeldeen, A.M. Negm, M.A. El Sawwaf, Evaluating the physical characteristics of biopolymer/soil mixtures, Arab. J. Geosci. 9 (2016) 371.

[15] H.R. Khatami, B.C. O'Kelly, Improving mechanical properties of sand using biopolymers, J. Geotech. Geoenviron. Eng. 139 (2013) 1402–1406.

[16] I. Chang, A.K. Prasidhi, J. Im, G.C, Cho. Soil strengthening using thermo-gelation biopolymers, Constr. Build. Mater. 77 (2015) 430–438.

[17] I. Chang, J. Im, G.C. Cho, Geotechnical engineering behaviors of gellan gum treated sand, Can. Geotech. J. 53 (2016) 1658-1670.

[18] I. Chang, J. Im, S.W. Lee, G.C. Cho, Strength durability of gellan gum biopolymer-treated Korean sand with cyclic wetting and drying, Constr. Build. Mater. 143 (2017) 210–221.

[19] I. Chang, G.C. Cho, Shear strength behavior and parameters of microbial gellan gum-treated soils: from sand to clay, Acta. Geotech. 14 (2019) 361–375.

[20] R. Aguilar, J. Nakamatsu, E. Ramírez, M. Elgegren, J. Ayarza, S. Kim, M.A. Pando, L.

Ortega-San-Martin, The potential use of chitosan as a biopolymer additive for enhanced mechanical properties and water resistance of earthen construction, Constr. Build. Mater. 114 (2016) 625–637.

[21] N. Hataf, P. Ghadir, N. Ranjbar, Investigation of soil stabilization using chitosan biopolymer, J. Clean Prod. 170 (2018) 1493–1500.

[22] J. Nakamatsu , S. Kim, J. Ayarza, E. Ramírez, M. Elgegren, R. Aguilar, Eco-friendly modification of earthen construction with carrageenan: Water durability and mechanical assessment, Constr. Build. Mater. 139 (2017) 193–202.

[23] H. Fatehi, S.M. Abtahi, H. Hashemolhosseini, S.M. Hejazi, A novel study on using protein-based biopolymers in soil strengthening, Constr. Build. Mater. 167 (2018) 813–821.

[24] I. Chang, J. Im, M.K. Chung, G.C. Cho, Bovine casein as a new soil strengthening binder from diary wastes, Constr. Build. Mater. 160 (2018) 1–9.

[25] P. Ghadir, N. Ranjbar, Clayey soil stabilization using geopolymer and Portland cement, Constr. Build. Mater. 188 (2018) 361-371.

[26] I. Chang, J. Im, A.K. Prasidhi, G.C. Cho, Effects of xanthan gum biopolymer on soil strengthening, Constr. Build. Mater. 74 (2015) 65–72.

[27] N. Latifi, S. Horpibulsuk, C.L. Meehan, M.Z.A. Majid, A.S.A. Rashid, Xanthan gum biopolymer: an eco-friendly additive for stabilization of tropical organic peat, Environ. Earth. Sci. 75 (2016) 825.

[28] G.C. Barrére, C.E. Barber, M.J. Daniels, Molecular cloning of genes involved in the production of the extracellular polysaccharide xanthan by *Xanthomonas campestris* pv. *campestris*, Int. J. Biol. Macromol. 8 (1986) 372–374.

[29] S. Rosalam, R. England, Review of xanthan gum production from unmodified starches by xanthomonas comprestris sp, Enzyme Microb. Technol. 39 (2) (2006) 197–207.

[30] C. Lam, S.A. Jefferis, The use of polymer solutions for deep excavations: lessons from Far Eastern experience. HKIE Transactions 21 (4) (2014) 262-271.

[31] C. Lam, S.A. Jefferis, Polymer Support Fluids in Civil Engineering, ICE, 2017.

[32] R. Guerrero-Lemus, J.M. Martinez-Duart, Renewable energies and $CO_2$: Cost Analysis, Environmental Impacts and Technological Trends, 2012 edition, Springer London, UK, 2013.

[33] H.B. Seed, C.K. Chan, Clay strength under earthquake loading conditions, J. Soil Mech. Found. Div. 92 (2) (1966) 53–78.

[34] J.P. Carter, J.R. Booker, C.P. Wroth, A critical state soil model for cyclic loading, Soil mechanics—Transient and cyclic loading (1982) 219–252.

[35] J.C. Chai, N. Miura, Traffic-load-induced permanent deformation of road on soft subsoil, J. Geotech. Geoenviron. Eng. 128 (11) (2002) 907–916.

[36] X. Geng, C. Xu, Y. Cai, Non-linear consolidation analysis of soil with variable compressibility and permeability under cyclic loadings, Int. J. Numer. Anal. Met. 30 (8) (2006) 803–821.

[37] K.H. Andersen, Bearing capacity under cyclic loading—offshore, along the coast, and on land, Can. Geotech. J. 46 (5) (2007) 513–535.

[38] J. Ni, I. Indraratna, X. Geng, J.P. Carter, Y. Chen, Model of soft soils under cyclic loading, Int. J. Geomech. 15 (4) (2015) 04014067 (10 pp.).

[39] Y. Cai, X. Geng, C. Xu, Solution of one-dimensional finite-strain consolidation of soil with variable compressibility under cyclic loadings, Comput. Geotech. 34 (1) (2007) 31-40.

[40] Y. Cai, X. Geng, Consolidation analysis of a semi-infinite transversely isotropic saturated soil under general time-varying loadings, Comput. Geotech. 36 (3) (2009) 484-492.

[41] J. Wang, Z. Gao, H. Fu, G. Ding, Y. Cai, X. Geng, C. Shi, Effect of surcharge loading rate and mobilized load ratio on the performance of vacuum–surcharge preloading with PVDs, Geotext. Geomembranes 47 (2) (2019) 121-127

[42] Y. Chen, J. Ni, P. Zheng, R. Azzam, Y. Zhou, W. Shao, Experimental research on the behaviour of high frequency fatigue in concrete, Eng. Fail Anal. 18 (2011) 1848–1857.

[43] Y. Chen, J. Ni, W. Shao, Y. Zhou, A. Javadi, R. Azzam, Coalescence of fractures under uni-axial compression and fatigue loading, Rock Mech. Rock. Eng. 45 (2012a) 241–249.

[44] Y. Chen, J. Ni, W. Shao, R. Azzam, Experimental study on the influence of temperature on the mechanical properties of granite under uni-axial compression and fatigue loading, Int. J. Rock Mech. Min. 56 (2012b) 62–66.

[45] B.M. Lekha, G. Sarang, A.U.R. Shankar, Effect of electrolyte lignin and fly ash in stabilizing black cotton soil, Transp. Infrastruct. Geotech. 2 (2015) 87–101.

[46] I. Chang, Y.M. Kwon, J. Im, G.C. Cho, Soil consistency and interparticle characteristics of xanthan gum biopolymer – containing soils with pore-fluid variation, Can. Geotech. J. 56 (8) (2019) 1206–1213.

[47] A. Soldo, M. Miletić, M.L. Auad, Biopolymers as a sustainable solution for the enhancement of soil mechanical properties, Sci. Rep-Uk. 10 (1) (2020) 213-267.

[48] A.S.A. Rashid, S. Tabatabaei, S. Horpibulsuk, N.Z. Mohd Yunus, W.H.W. Hassan, Shear Strength Improvement of Lateritic Soil Stabilized by Biopolymer Based Stabilizer, Geotechnical and Geological Engineering 37 (6) (2019) 5533-5541.

[49] S. Smitha, K. Rangaswamy, D.S. Keerthi, Triaxial test behaviour of silty sands treated with agar biopolymer, International Journal of Geotechnical Engineering (2019) 1-12.

[50] M.G. Arab, A.M. ASCE, R.A. Mousa, A.R. Gabr, A.M. Azam, S.M. El-Badawy, A.F. Hassan, Resilient behavior of sodium alginate – treated cohesive soils for pavement applications, J. Mater. Civ. Eng. 91 (3) (2019) 04018361.

[51] A.F. Cabalar, M.H. Awraheem, M.M. Khalaf, Geotechnical properties of a low-plasticity clay with biopolymer, J. Mater. Civ. Eng. 30 (8) (2018) 4018170.

**List of Tables**



**Table 1** Basic engineering properties of Shanghai clay

| Properties | Values |
|---|---|
| Proctor compaction test | |
| Optimum moisture content (OMC),% | 23 |
| Maximum dry density ($\rho_{dmax}$), g/cm$^3$ | 1.59 |
| Gravimetric-volumetric parameters | |
| Unit weight ($\gamma$), kN/m$^3$ | 17.3 |
| Specific gravity ($G_s$) | 2.73 |
| Natural water content ($\omega$), % | 42.7 |
| Natural void ratio | 1.21 |
| Degree of saturation ($S_r$), % | 96 |

**Table 2** Test matrix for standard proctor compaction, Atterberg limit and unconfined compression strength tests

| Test | Xanthan gum-to-soil ratio ($m_b/m_s$), % | Initial moisture content ($m_w/(m_b+m_s)$), % |
|---|---|---|
| Standard proctor compaction test | 1.0, 2.0, 3.0, 4.0, 5.0 | -- |
| Atterberg limit test ($w_P$ and $w_L$) | 1.0, 2.0, 3.0, 4.0, 5.0 | -- |
| Unconfined compression strength test | 1.0, 2.0, 3.0, 4.0, 5.0 | 23, 26, 28, 30, 32 |

**Table 3** Test matrix of constant-amplitude fatigue loading tests

| $m_b/m_s$, % | $\sigma_m$/UCS | $\sigma_a$/UCS | $\sigma_{max}$/UCS | $\sigma_{min}$/UCS | Number of cycles at failure ($N_f$) |
|---|---|---|---|---|---|
| 0.0 | 0.3 | 0.25 | 0.55 | 0.1 | 233,750 |
| 0.0 | 0.65 | 0.1 | 0.75 | 0.55 | 38,584 |
| 1.0 | 0.4 | 0.15 | 0.55 | 0.25 | 1,256,247 |
| 1.0 | 0.4 | 0.3 | 0.7 | 0.1 | 377,524 |
| 2.0 | 0.4 | 0.15 | 0.55 | 0.25 | 1,945,328 |
| 2.0 | 0.6 | 0.15 | 0.75 | 0.45 | 525,271 |
| 3.0 | 0.4 | 0.3 | 0.7 | 0.1 | 16,375,364 |
| 3.0 | 0.55 | 0.15 | 0.7 | 0.4 | 1,386,072 |

**Table 4** Test matrix of stepping-amplitude fatigue loading tests

| $m_b/m_s$, % | $\sigma_m$/ UCS | $\sigma_a$/UCS | $\sigma_{max}$/UCS | $\sigma_{min}$/ UCS | Number of cycles at failure ($N$) |
|---|---|---|---|---|---|
| 0.0 | 0.45 | 0. 05 | 0.5 | 0.4 | 500,000 |
| | | 0.15 | 0.6 | 0.3 | 6,235 |
| | | 0.25 | 0.7 | 0.2 | -- |
| | | 0.35 | 0.8 | 0.1 | -- |
| 1.0 | 0.45 | 0. 05 | 0.5 | 0.4 | 500,000 |
| | | 0.15 | 0.6 | 0.3 | 500,000 |
| | | 0.25 | 0.7 | 0.2 | 142,587 |
| | | 0.35 | 0.8 | 0.1 | -- |
| 2.0 | 0.45 | 0. 05 | 0.5 | 0.4 | 500,000 |
| | | 0.15 | 0.6 | 0.3 | 500,000 |
| | | 0.25 | 0.7 | 0.2 | 500,000 |
| | | 0.35 | 0.8 | 0.1 | 95,547 |
| 3.0 | 0.45 | 0. 05 | 0.5 | 0.4 | 500,000 |
| | | 0.15 | 0.6 | 0.3 | 500,000 |
| | | 0.25 | 0.7 | 0.2 | 500,000 |
| | | 0.35 | 0.8 | 0.1 | 215,869 |

**List of Figures**

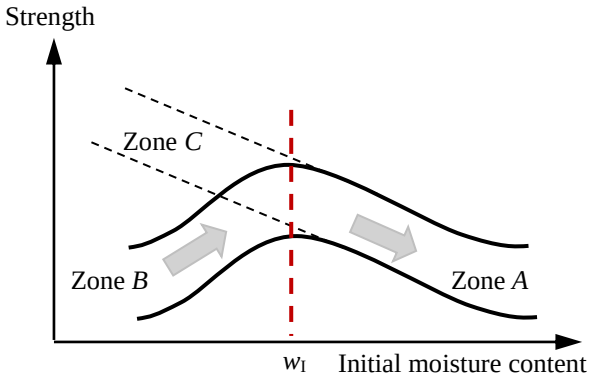


**Fig. 1.** Variation of strength with initial moisture content for biopolymer-treated soils.

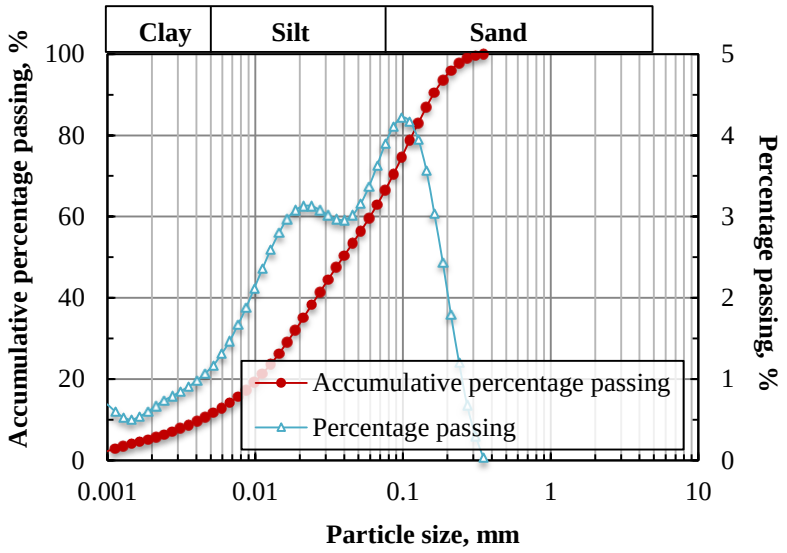


**Fig. 2.** Particle size distribution curve of Shanghai clay.

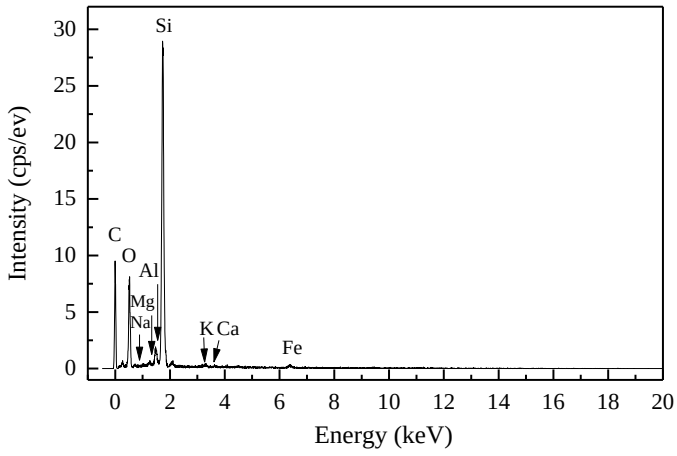


**Fig. 3.** Chemical analysis of Shanghai clay (X-ray Fluorescence spectrum).

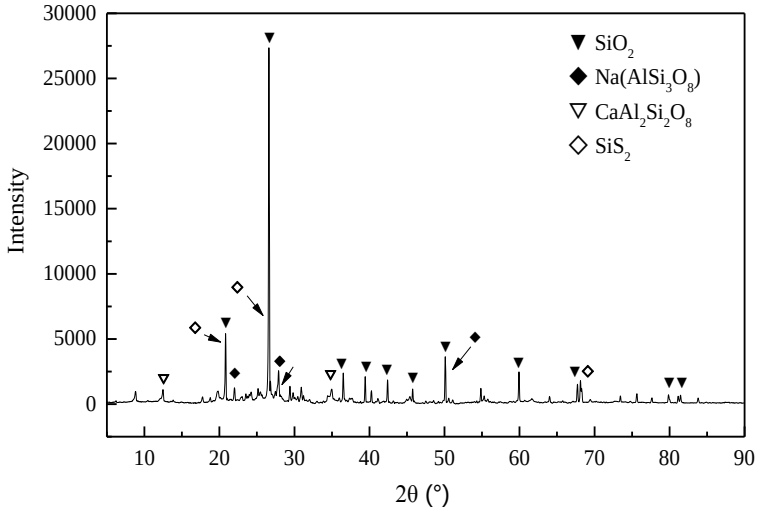


**Fig. 4.** Mineralogical analysis of Shanghai clay (X-ray powder diffraction pattern).

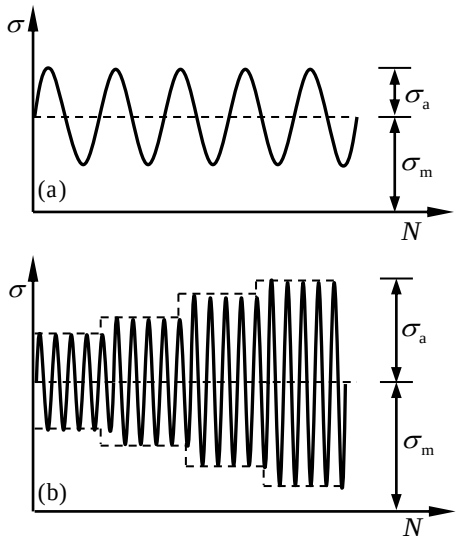


**Fig. 5.** Loading schemes for (a) constant-amplitude and; (b) stepping-amplitude fatigue loading tests.

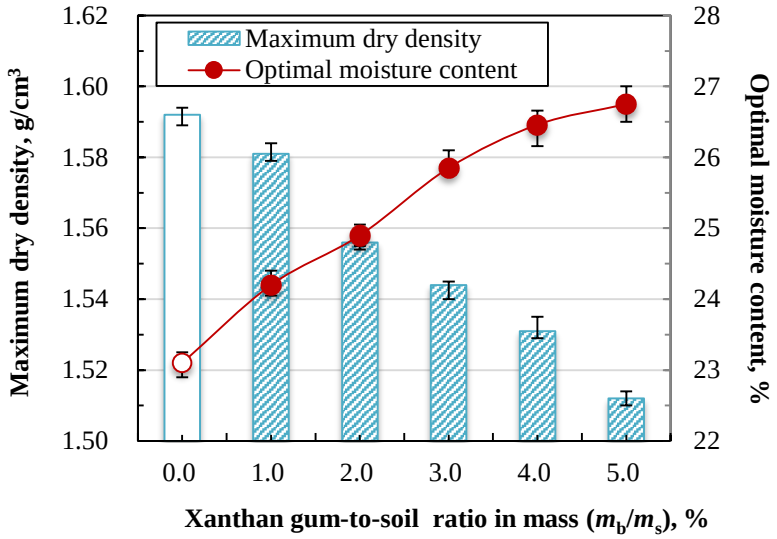


**Fig.6.** Variation of maximum dry density and optimal moisture content versus biopolymer contents.

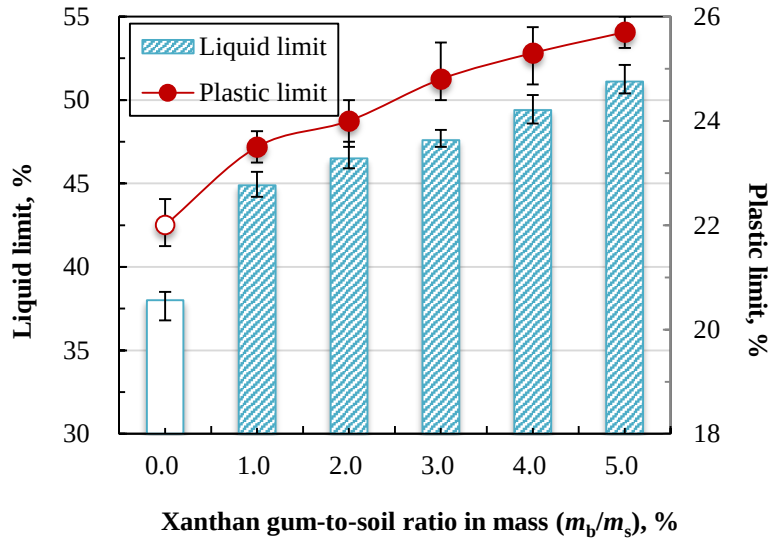


**Fig. 7.** Variation of liquid limit and plastic limit versus biopolymer contents.

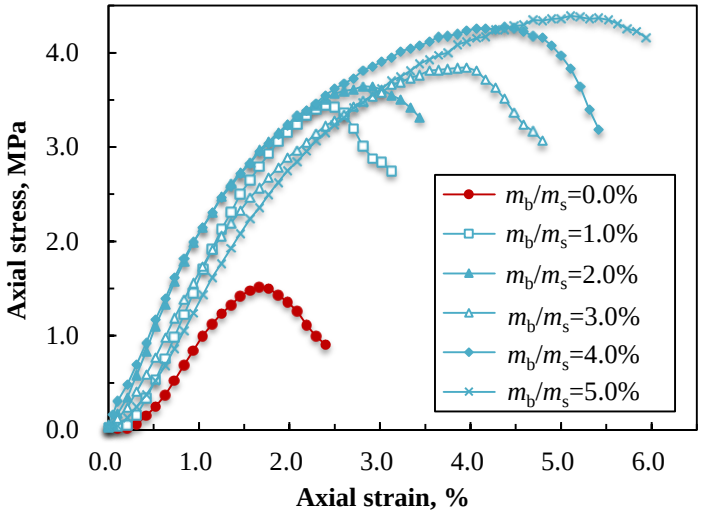


**Fig. 8.** Stress-strain curves for different xanthan gum contents ($w$= 30%).

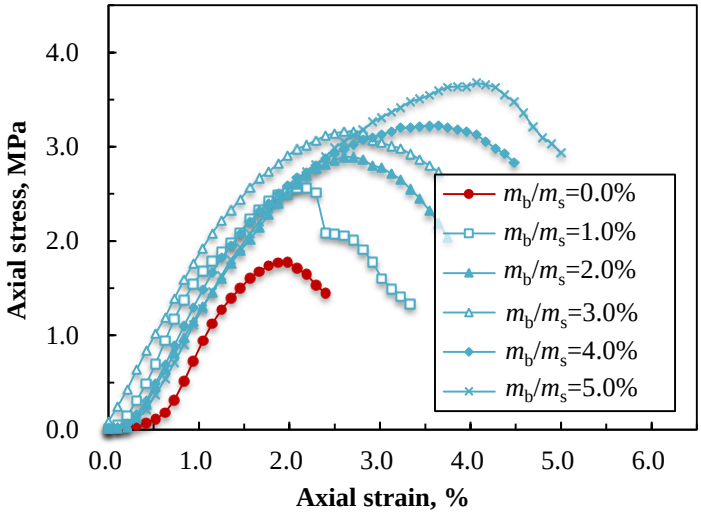


**Fig. 9.** Stress-strain curves for different xanthan gum contents ($w$= 26%).

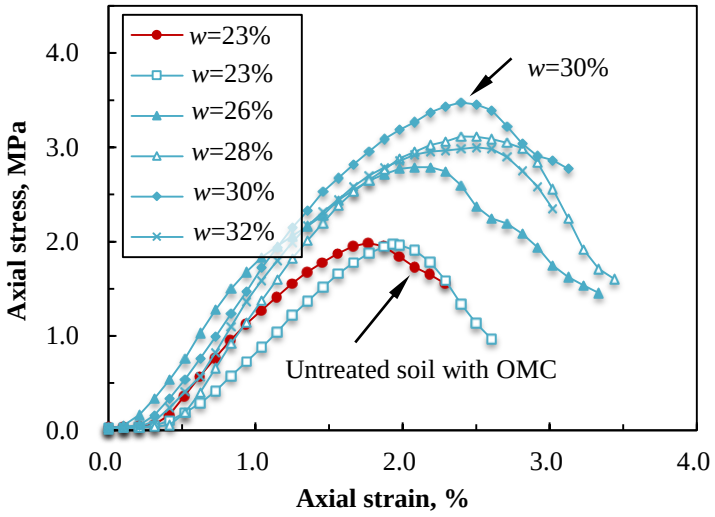


**Fig. 10.** Stress-strain curves for different initial moisture contents ($m_b/m_s$= 1.0%).

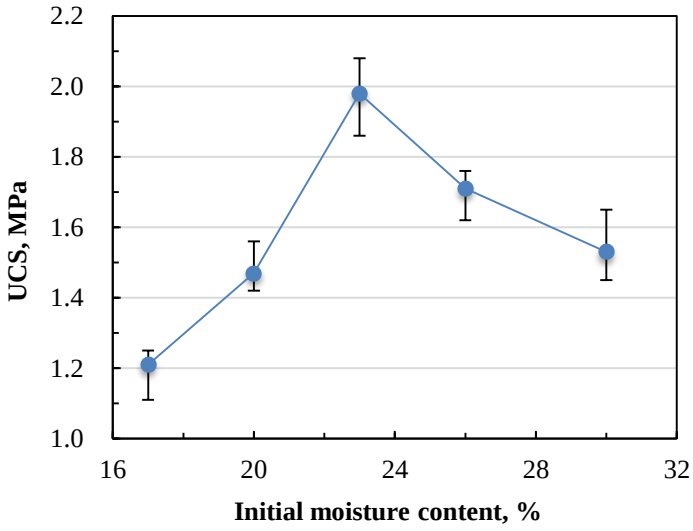


**Fig. 11.** Variation of UCS versus initial moisture content ($m_w/(m_s+m_b)$) for untreated soils.

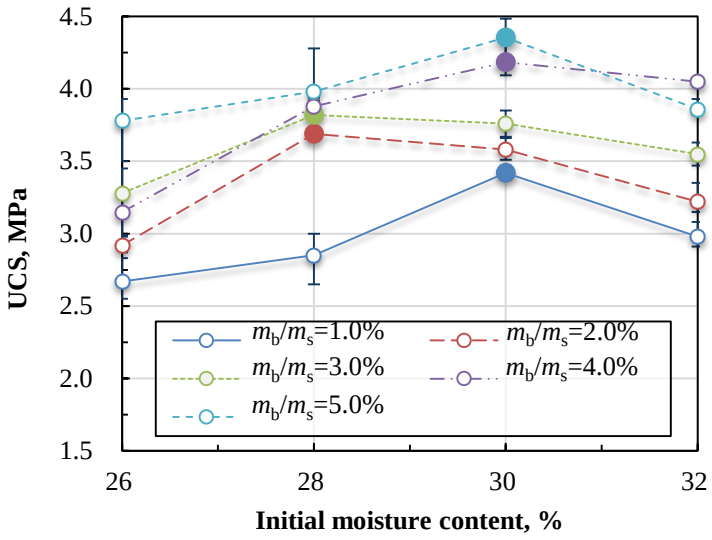


**Fig. 12.** Variation of UCS versus initial moisture contents ($m_w/(m_s+m_b)$) for biopolymer-treated soils.

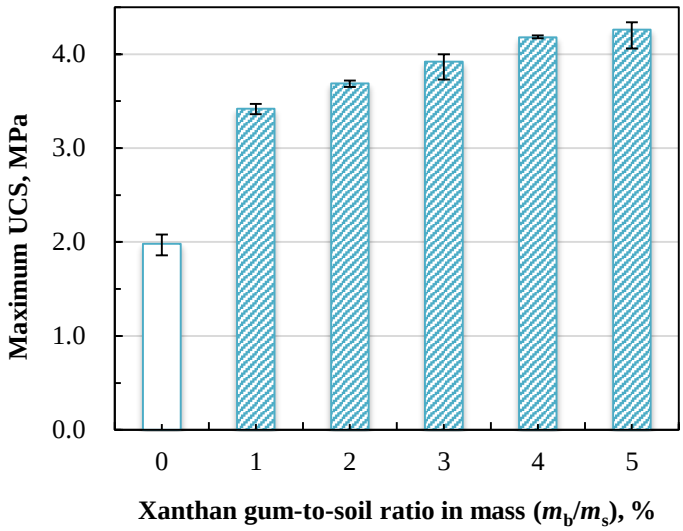


**Fig. 13.** Maximum UCS for five biopolymer contents at the ideal initial moisture contents.

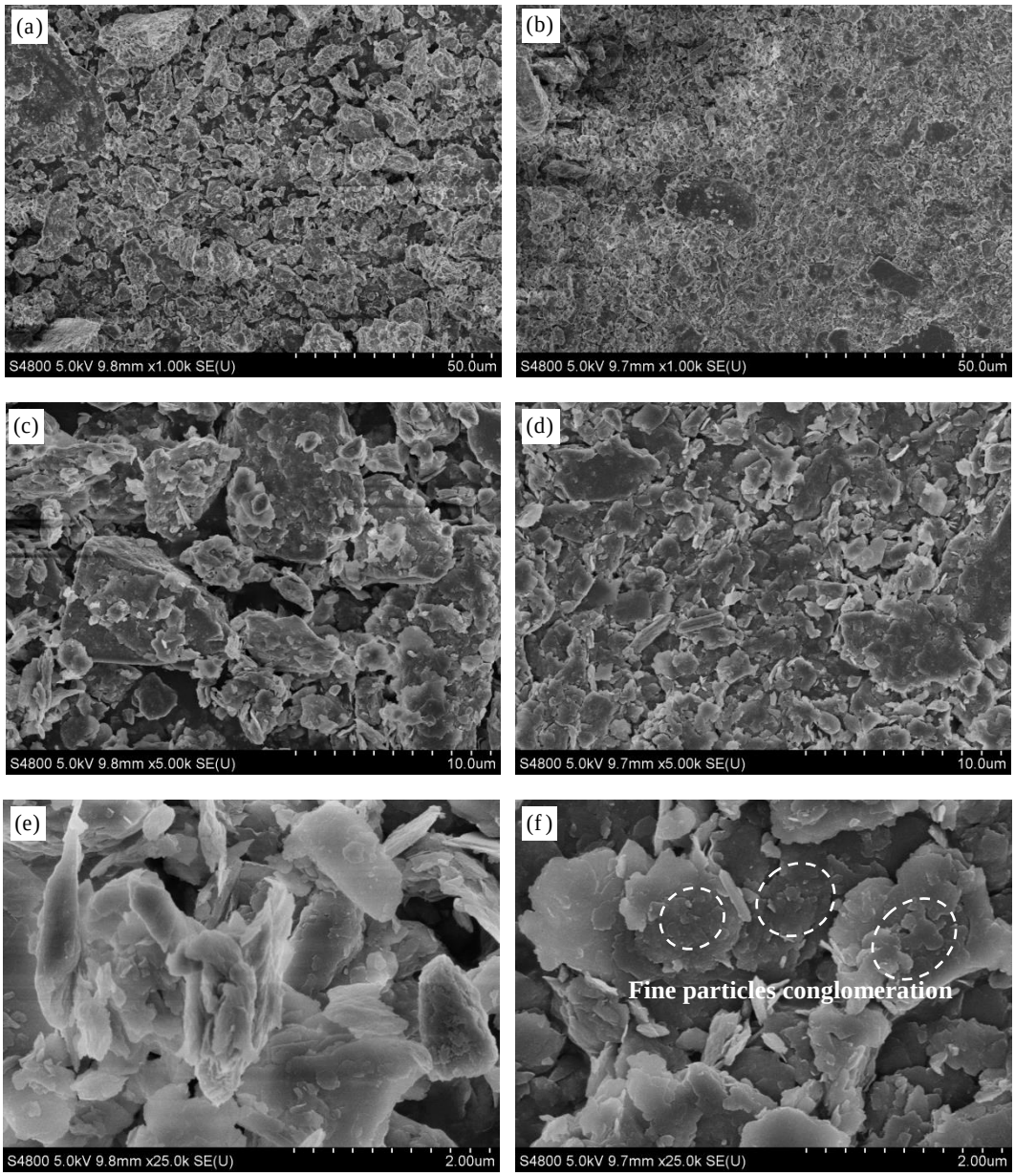


**Fig. 14.** SEM images of untreated soils (a), (c), and (e); and xanthan gum-treated soils (b), (d) and (f).

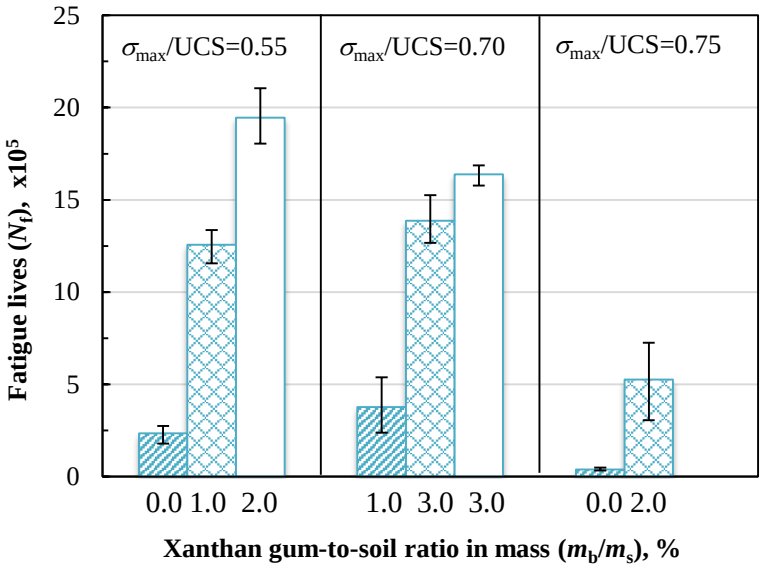


**Fig. 15.** Variation of Fatigue lives with $m_b/m_s$ and $\sigma_{max}$/UCS.

**Manuscript Number:** CONBUILDMAT-D-19-10101

**Title:** Performance of soils enhanced with eco-friendly biopolymers in unconfined compression strength tests and fatigue loading tests

**Authors:** Jing Ni, Shan-Shan Li, Lei Ma, Xue-Yu Geng

# Response to Editor:

Reviewers have now commented on your paper. You will see that they are advising that you revise your manuscript. If you are prepared to undertake the work required, I would be pleased to consider your paper for publication.

Response: We would like to wholeheartedly thank you very much for your time, patience, and efforts during the process. At the same time, we would like to thank the reviewers for their time, patience, and constructive criticism. We found that the reviewers' comments are very valuable for us. We have revised the manuscript to address the reviewers' comments. Please do not hesitate to contact us if anything needs to be clarified further.

# Response to Reviewer #4:

The authors thank the reviewer for the suggestive comments. The paper has been improved according to your comments. In the revised version, all the revised contents are marked with red color. Detailed revisions are listed as follows:

1. Although this is a laboratory study, the authors are encouraged to briefly discuss how soft clay can be treated with xanthan gum in practice. In other words, please discuss how xanthan gum can be mixed with soft clay on a site (e.g. deep mixing by auger, or by grouting, etc.) and the way of mixing (dry mix, wet mix?). This information is important for the actual application of this new material/technique.

   Response:

   The possible implementations of xanthan gum treatment in geotechnical engineering practices have been added in the Section 3.5. Please see Page 15, Lines 388 to 390 and Page 16, Lines 391 to 406.

   The incorporation of xanthan gum into soils on site can be conducted through deep

mixing, spraying, grouting, high-pressure injection, and etc. [1-3]. Given the high viscosity of xanthan gum solution that is prone to block the voids in soils for further solution penetration, deep mixing might be recommended. In the existing laboratory research, biopolymers have been introduced into the soil in power or solution form (i.e., dry mixing or wet mixing). According to Arab et al. [4], wet mixing method is more effective in treating different cohesive soils with sodium alginate. Ayeldeen et al. [5] observed that the efficiency of xanthan gum or guar gum through wet mixing in reducing collapsibility was about 2-3 times more than dry mixing, while Chang et al. [6] reported that dry mixing is more effective than wet mixing by providing a well-distributed xanthan matrix in soil given that the amount of mixing water is sufficient for xanthan gum dissolution. As for practical applications, dry mixing is considered as an appropriate method [7]. Therefore, the choice of mixing method in practice may need to be determined according to the solubility, the addition amount and types of biopolymers, and soil types. Furthermore, various factors such as workability, construction cost, relevant machinery, and environmental issue need to be assessed for practical and economic application on site.

# Reference:


[1] I. Chang, J. Im, G.C. Cho, Introduction of microbial biopolymers in soil treatment for future environmentally-friendly and sustainable geotechnical engineering, Sustain 8 (251) (2016) 1–23.

[2] C. Lam, S.A. Jefferis, Polymer Support Fluids in Civil Engineering, ICE, 2017.

[3] S. Smitha, K. Rangaswamy, D.S. Keerthi, Triaxial test behaviour of silty sands treated with agar biopolymer, International Journal of Geotechnical Engineering (2019) 1-12.

[4] M.G. Arab, A.M. ASCE, R.A. Mousa, A.R. Gabr, A.M. Azam, S.M. El-Badawy, A.F. Hassan, Resilient behavior of sodium alginate – treated cohesive soils for pavement applications, J. Mater. Civ. Eng. 91 (3) (2019) 04018361.

[5] M.K. Ayeldeen, A.M. Negm, M.A. El Sawwaf, Evaluating the physical characteristics of biopolymer/soil mixtures, Arab. J. Geosci. 9 (2016) 371.

[6] I. Chang, J. Im, A.K. Prasidhi, G.C. Cho, Effects of xanthan gum biopolymer on soil

strengthening, Constr. Build. Mater. 74 (2015a) 65–72.

[7] A.F. Cabalar, M.H. Awraheem, M.M. Khalaf, Geotechnical properties of a low-plasticity clay with biopolymer, J. Mater. Civ. Eng. 30 (8) (2018) 4018170.

HIGHLIGHTS

- Xanthan gum was used to treat Shanghai clay in this study.
- The effect of initial moisture content on performances of xanthan gum-treated soils was studied.
- There existed an ideal initial moisture content leading to the maximum UCS.
- Xanthan gum has the potential to stabilize soils under repeated loads.

*Declaration of Interest Statement

**Declaration of interests**

☒ The authors declare that they have no known competing financial interests or personal relationships that could have appeared to influence the work reported in this paper.

☐The authors declare the following financial interests/personal relationships which may be considered as potential competing interests:

**Credit author statement**

**Jing Ni:** Conceptualization, Methodology, Formal analysis, Writing - Original Draft, Supervision, Project administration, Funding acquisition.

**Shan-Shan Li:** Validation, Investigation, Writing - Original Draft.

**Ma Lei:** Validation, Investigation, Writing - Original Draft.

**Xue-Yu Geng:** Writing - Review & Editing.

# Performance of soils enhanced with eco-friendly biopolymers in unconfined compression strength tests and fatigue loading tests

**Jing Ni[a], Shan-Shan Li[a], Lei Ma[a], Xue-Yu Geng[b,*]**

[a]*Department of Civil Engineering, University of Shanghai for Science and Technology, 200093 Shanghai, P.R. China.*

[b]*School of Engineering, University of Warwick, Coventry, CV4 7AL, UK (*corresponding author)*

***Corresponding author**: Xue-Yu Geng (Email: xueyu.geng@warwick.ac.uk)

# Performance of soils enhanced with eco-friendly biopolymers in unconfined compression strength tests and fatigue loading tests

**Jing Ni[a], Shan-Shan Li[a], Lei Ma[a], Xue-Yu Geng[b,*]**

[a]*Department of Civil Engineering, University of Shanghai for Science and Technology, 200093 Shanghai, P.R. China.*

[b]*School of Engineering, University of Warwick, Coventry, CV4 7AL, UK (*corresponding author)*

***Corresponding author**: Xue-Yu Geng (Email: xueyu.geng@warwick.ac.uk)

**Abstract** Recently, biopolymers have emerged in soil stabilisation. The efficiency of biopolymers in ground improvement is mainly dependent on biopolymer types, soil types, biopolymer contents, curing periods, thermal treatment and mixing methods. However, the effect of the initial moisture content during sample preparation stages, on the mechanical behaviours of biopolymer-treated soils, has not been fully understood. The first part of this study probed the role of initial moisture content, in treating Shanghai clay with the xanthan gum by performing standard proctor compaction tests, Atterberg limit tests, unconfined compression strength (UCS) tests and microstructural analysis, while the second part contributed to capture the fatigue behaviours of the samples treated with an ideal moisture content by performing constant-amplitude and stepping-amplitude fatigue loading tests. Our results showed that the improvement appeared to occur from an average optimum moisture content for the treated soils (treated optimum), which was 3% wet of the untreated optimum. As the initial moisture content increased, the UCS values were elevated. However, there existed an ideal initial moisture content leading to the maximum strengthening efficiency. For xanthan gum content (i.e., the mass of xanthan gum with respect to the mass of dry soil) ranging from 1.0% to 5.0%, this ideal value was between 1.1 and 1.2 times the treated optimum. Our results also indicated that xanthan gum, as a biopolymer soil strengthener, was efficient in increasing either fatigue life or bearing capacity, under repeated loading for xanthan gum-soil matrices, when compared to untreated soils. While the untreated soils failed at the stress level of only half the UCS, the xanthan gum-treated soils with a 3.0% xanthan gum content sustained at the end of the tests. These data imply the potential use of xanthan gum in soil stabilisation, under repeated loads.

**Keywords** Xanthan gum, Initial moisture content, Unconfined compression strength, Repeated loads, Ground improvement

## 1. Introduction

During the past two decades, the application of biological processes to soil stabilisation has emerged in geotechnical engineering [1, 2]. Bio-mineralisation, which leads to mineral precipitation using the bio-technological mediation route, has been extensively investigated as a bio-treatment for soils [3-8]. More recently, the direct use of biogenic excrement (i.e., biopolymers) as a ground improvement method has gained increased academic interest, as biopolymers are abundant in nature and are considered eco-friendly materials for soil treatment [9], and on the other hand able to improve soil strength, even under a very low biopolymer-to-soil ratio (e.g., 0.5%) [10-12].

As a commonly applied contemporary biopolymer type in various practices, polysaccharides have been evaluated for their capacity to treat soils. Beta-glucan ($\beta$-1, 3/1, 6-glucan) and guar gum have been found operational and effective in enhancing the mechanical strength of soils [13, 14]. Gellan gum and agar gum have similar properties, including thermos-gelation and significant efficiency in strengthening soils [15-19]. The application of carrageenan and chitosan as additives to earthen constructions contributes positively on water durability [20-22]. In addition to polysaccharides, the incorporation of protein-based biopolymers (e.g., casein and sodium caseinate salt) to improve the mechanical properties and durability of natural soils has also been reported [23, 24].

Throughout the literature, it has been recognized that the efficiency of biopolymers in ground improvement is mainly dependent on biopolymer types, soil types, biopolymer contents, curing periods, thermal treatment and mixing methods. The effect of the moisture content on the performance of biopolymer-treated soils, however, has not been fully understood. Some researchers have revealed that the biopolymer-treated soils [12, 24], like other geopolymer-treated soils [25], appear to have a higher mechanical strength with a lower value of moisture content. During the sample preparation stage, a reduction in the initial moisture content may lead to an increased strength [19], which is illustrated in Fig. 1 (Zone

*A*). However, the strength is unlikely to continue increasing when the initial moisture content decreases (Fig. 1, Zone *C*), as too little water results in a poorly dissolved biopolymer solution, which could adversely affect the workability of the biopolymer-soil matrix and its consequent mechanical strength [26]. As a result, there might exist an ideal initial moisture content ($w_I$) leading to the highest strength as illustrated in Fig. 1, i.e., inflection point from Zone *B* to Zone *A*. Therefore, the initial moisture content appears to play an important role in the efficiency of soil treatment. Up to now, little research has been performed in this area. Usually, the initial moisture content has been set as a fixed value, e.g., liquid limit [13, 16, 26], optimum moisture content [21, 23], and natural moisture content [27].

In this study, the effect of the initial moisture content on the efficiency of soil treatment will be probed by an experimental study on the xanthan gum-treated Shanghai clay. Xanthan gum has been extensively researched in the soil treatment due to its unique functional properties. It has excellent cold water dissolving capacity, pH stability, storage stability, ionic salt compatibility, and pseudo-plastic flow characteristics [28, 29]. For geotechnical engineering, xanthan gum has been used as polymer support fluids to stabilize deep excavations [30, 31]. Recent studies have reported that xanthan gum, providing bonds between soil particles, has the potential to act as a soil strengthener [12, 14, 26, 27]. In addition, the presence of xanthan gum in soils reduces the hydraulic conductivity due to the "clogging effect", and enables hydrogen bonds to enhance the strength and corrosion resistance of sands [14, 26, 27].

On the other hand, xanthan gum are available at reasonable prices. In general, the market prices of biopolymers are more expensive than conventional soil stabilizers and inorganic binders (e.g., geopolymers). However, taken into account the global greenhouse gas reduction efforts (e.g., carbon emission trading), biopolymers will become remarkably competitive in soil treatment, e.g., for a unit amount (1 ton) of soil treatment, 0.5% xanthan gum is only 3.6% more expensive than 10% cement [9, 32]. In addition, the biopolymers have higher production

costs due to their widespread use in the fields of food production, agriculture, and medical treatment. For geotechnical applications, it is expected that the price of biopolymers will be greatly reduced due to the unnecessary edible standards [9, 14].

To the authors' knowledge, limited research has accessed the fatigue behaviours of the xanthan gum-treated soils. Soils subjected to repeated loads can fail under a stress level consisting only a fraction of a static strength [33-41]. Therefore, a lack of understanding of the mechanical behaviours of the biopolymer-treated soils under fatigue loading will restrict the evaluation of their long-term resilience and practical engineering performances (e.g., highway pavements, railway tracks, and airport runways). Given this background, this study involved investigating the performances of xanthan gum-treated soils from two aspects, i.e., the ideal treatment condition (e.g., ideal initial moisture content) to achieve the maximum strengthening effect and fatigue behaviours under the ideal treatment condition. Standard proctor compaction tests and Atterberg limit tests were also performed along with the SEM images to better understand the underlying strengthening mechanisms.

## 2. Materials and Methods

### *2.1. Shanghai clay*

Shanghai lies in the Yangtze River delta alluvial plain in China. For this study, natural soils were sampled from a construction site of Metro Line 15 in the northwest Shanghai, at a depth of 8.9 m. Table 1 shows some of the basic engineering properties for Shanghai clay, e.g., optimum moisture content (OMC) and maximum dry density ($\rho_{dmax}$), and gravimetric-volumetric parameters.

Particle size distribution analysis was performed on the soil using a Mastersizer 3000 particle size analyser (Malvern, UK), which caters for the particles in the range of 10 nm to 3.5 mm. As shown in Fig. 2, the natural soil had 33.41% by weight sand content, 54.86% silt

content, and 11.73% clay content based on the soil particle size ranges as recommended in ASTM D422. The Atterberg limits, i.e., the liquid and plastic limits of the natural soil, were found to be $w_L$=37.9% and $w_P$=22%, respectively. The corresponding plastic index was $I_P$=15.9%. Combined with the particle size distribution curve and Atterberg limits, the natural soil was therefore classified as sand lean clay, as per ASTM D2487.

An X-ray fluorescence (XRF) test on the soil was performed using a portable QUANTAX energy-dispersive X-ray microanalysis (EDX) spectrometer (Brucker, Germany), equipped with a 2.5 kg probe, 50 W pulse processor and Esprit analysis software. The XRF spectrum (Fig. 3) indicated that the most abundant elements were Si, C, O, Al, K, Mg, Na, and Fe.

Mineralogical analysis of the natural soil was conducted using the X-ray powder diffraction test (XRPD), using a D8 ADVANCE diffractometer (Brucker, Germany). Data was automatically collected for phase angles ($2\theta$), ranging between 5º and 90º, at 0.02º intervals. Identification of the crystalline phases was carried out using JADE software. XRPD patterns are shown in Fig. 4, including main peak identification, $SiO_2$.

### *2.2. Xanthan gum*

Xanthan gum is a polysaccharide formed by the fermentation of sugar (e.g., glucose or sucrose) by the bacterium *Xanthomonas campestris.* It was chosen to treat Shanghai clay for its unique functional properties and reasonable prices as previously demonstrated. The xanthan gum powder for this study was manufactured by Shandong Fengtai Biological Technology Co., Ltd.

### *2.3. Sample fabrication*

Sample preparation for both unconfined compression strength tests and fatigue loading tests followed the same procedures. The Shanghai clay was oven dried (105 ºC) for 24 hours,

broken down carefully with rubber hammers, and sieved using a 2 mm sieve to obtain a base soil. The base soil was thoroughly mixed with xanthan gum, before distilled water was added. To increase the solubility, the distilled water was heated to 80 ºC [26]. A metal trowel was used for mixing manually for about five minutes until a homogeneous xanthan gum-soil mixture was obtained. The mixture was then placed inside a cylindrical mould with an inner diameter of 39.1 mm and a height of 80 mm in three layers. For each layer, 25 blows were applied through a rammer (305.5 g) dropping from a height of 247 mm. The compacted samples were extruded after compaction, and cured in a controlled environment at 60% relative humidity and 20 ºC for 28 days.

### 2.4 *Experimental programme*

The experimental program involved exploring the influence of using xanthan gum on the behaviours of Shanghai clay from five aspects: (1) compaction properties; (2) Atterberg limits; (3) microscopic structures; (4) mechanical properties under unconfined compression and (5) fatigue loading. The following subsections present the test procedures for each component of the experimental programme. Each test was replicated at least three times to achieve a reliable average.

#### *2.4.1* Standard proctor compaction tests

The standard proctor compaction tests were conducted in accordance with ASTM D698 to determine the maximum dry density and its corresponding optimum moisture content for xanthan gum-treated soil samples. Five xanthan gum contents (the mass of xanthan gum with respect to the mass of dry soil), e.g., $m_b/m_s$=1.0%, 2.0%, 3.0%, 4.0%, and 5.0% (Table 2), were used to investigate the variation of compaction properties with the increasing xanthan gum content.

#### *2.4.2* Atterberg limit tests

The Atterberg limits ($w_P$ and $w_L$) of the soils treated with five xanthan gum contents (Table 2) were determined by Liquid-Plastic Limit Combined Test (GB/T 50123-2019, Part 9) by using a cone with a mass of 76 g and a tip angle of 30°. The penetration depth of the cone into the sample (55 mm diameter and 40 mm height) was measured 5 s after the cone had been released. For each biopolymer content, the test was repeated on five samples with an increased moisture content. The water contents corresponding to 17 mm and 2 mm determined with the aid of a linear fitting curve in the semi-log plane of cone penetration-moisture content were regarded as liquid limit and plastic limit, respectively.

### *2.4.3.* Unconfined compression strength tests

The effectiveness of incorporating xanthan gum in improving the soil strength at different initial moisture contents was investigated by the unconfined compression strength tests, which were conducted under the strain-controlled condition at a loading rate of 1.5%/min in accordance with ASTM D2166. The xanthan gum contents used were the same as those adopted for the standard proctor compaction and Atterberg limit tests. For each biopolymer content, five initial moisture contents were employed (Table 2). As suggested by Fatehi et al. [23] and Hataf et al. [21], the optimum moisture content of the untreated soil ($w$=23%) (hereafter referred as untreated optimum) was adopted as the minimum initial moisture content. The xanthan gum-treated soil samples with $w$=23% had a lot of voids on the sample surfaces, indicating an unthorough mixing due to the poor workability of the xanthan gum-soil mixture. Then 3% wet of the untreated optimum was selected based on the results of the standard proctor compaction tests (section 2.4.1), which indicated that the mean value of the optimum moisture contents of the treated soils (hereafter referred as treated optimum) with various xanthan gum contents was $w$=26%. Afterwards, the initial moisture content was increased at an interval of 2%. With the increment in the amount of water for sample mixing, the workability of the xanthan gum-soil mixture was improved. However, as the initial moisture content reached 34%, the compacted samples were visually deformed after they

were extruded from the cylindrical mould. Therefore, $w$=32% was adopted as the maximum initial moisture content. The untreated soil sample, prepared with the optimum moisture content $w$=23%, served as a control sample.

### *2.4.4. Fatigue loading tests*

Apart from the unconfined compression strength tests, fatigue loading tests were performed on the xanthan gum-treated soil samples as well. These samples used $w$=30%, and $m_b/m_s$ = 1.0%, 2.0%, and 3.0%. They were cured under the controlled conditions for 28 days before being exposed to the fatigue loading tests. The ZWICK-100HFP5100 test apparatus (ZwickRoell, Germany) was employed to apply fatigue loads. For detailed descriptions see Chen et al. [42-44]. The test procedure started with the mounting of cylindrical samples on the loading frame and bringing the load cell into contact with the sample surface. Through the user-friendly visualisation window, the mean stress, stress amplitude, and maximum loading cycles were fed into the load application device. The loading system was switched on at the same time as the automatic data acquisition system, and fatigue loading was initiated. The process continued until failure of the sample, or the maximum loading cycle was reached.

In this study, the fatigue loading tests involved two strategies: constant-amplitude and stepping-amplitude. In the constant-amplitude tests, the mean stress ($\sigma_m$) and stress amplitude ($\sigma_a$) for each sample remained constant during the loading process. In the stepping-amplitude tests, the mean stress remained constant, but the stress amplitude increased stepwise. Details of the two components of fatigue loading test are described as follows.

The loading schemes for the constant-amplitude and stepping-amplitude fatigue loading tests are shown in Fig. 5. The test input parameters included the mean stress($\sigma_m$) and stress amplitude ($\sigma_a$). The corresponding maximum stress ($\sigma_{max}=\sigma_m+\sigma_a$) and the minimum stress ($\sigma_{min}=\sigma_m-\sigma_a$) were calculated. The effects of $\sigma_m$, $\sigma_a$ and their combination on fatigue life were investigated. The test matrix of constant-amplitude fatigue loading tests is given in Table 3.

The maximum stress were from 1/2 to 3/4 fractions of UCS values referring to Lekha et al. [45], corresponding to medium to high stress levels. The UCS for each treatment condition was used as a basis for the calculation of fatigue stresses (e.g., $\sigma_m$, $\sigma_a$, $\sigma_{max}$, and $\sigma_{min}$). The maximum number of loading cycles for each test was set as 2,000,000. The loading frequency was set as a resonant frequency between the sample and the apparatus, which was about 40 to 45 Hz, rather than a fixed value.

For the stepping-amplitude fatigue loading tests, the mean stress ($\sigma_m$) for each sample was constant, while the stress amplitude ($\sigma_a$) increased step by step, at a constant interval. For each loading step, 500,000 cycles of fatigue loading were applied. The fatigue loading tests started from the first step and stopped until either the designed number of cycles was reached, or the sample failed. The test matrix of the stepping-amplitude fatigue loading tests are given in Table 4.

#### *2.4.5. Microscopic structures*

Scanning electrons microscope (SEM) and field emission scanning electron microscope (FESEM) have been used to explore the microstructural characteristics of biopolymer-treated soils, including shapes, sizes, and aggregation of soil particles [19, 23, 27]. In this study, SEM images were taken for both untreated soils and xanthan gum-treated soils ($m_b/m_s$=1.5% and $w$=28%). Microstructural analysis was conducted to better understand the connection between xanthan gum and Shanghai clay, and furthermore the underlying mechanisms of soil stabilization.

## *3. Results and discussion*

### *3.1 Effect of biopolymer contents on compaction characteristics*

The introduction of xanthan gum altered the compaction characteristics of Shanghai clay. The optimum moisture content was observed to increase from 23% to 26.7%. and the

maximum dry density had a descending trend falling from 1.59 g/cm$^3$ to 1.51 g/cm$^3$, as the xanthan gum content increased from $m_b/m_s$= 0.0% to 5.0% (Fig. 6). Ayeldeen et al. [14] reported that this alteration may depend on both the biopolymer characteristics (e.g., chemical properties and solution viscosities) and soil fine-grained content. In the current study, xanthan gum molecules contain a large number of hydrophilic groups (e.g., -OH and -COOH) and therefore have a large capacity to attract water molecules or dissolve in water, and retain water. As a result, elevating the xanthan gum content increased the amount of absorbed water, and therefore increased the optimum moisture content and decreased the maximum dry density.

### *3.2 Effect of biopolymer contents on Atterberg limits*

The liquid limit increased obviously from 37.9% to 44.9% as the $m_b/m_s$ ratio increased from 0.0% to 1.0%, and then slightly increased with the increasing xanthan gum content, to a maximum value of 51.1% at $m_b/m_s$= 5.0%, as shown in Fig. 7. The increasing trend of liquid limit of xanthan gum-soil matrix was also observed by Chang et al. [46]. The mechanism responsible for this phenomenon is similar to that works in compacting xanthan gum-treated soil (e.g., hydrophilic properties and water retention capacity). Treated samples with a higher xanthan gum content had a higher content of hydrophilic xanthan gum hydrogel, leading to a higher liquid limit. Simultaneously, the plastic limit increased gradually from 22% to 25.7% as the xanthan gum content increased from 0.0% to 5.0%.

### *3.3. Results of unconfined compression strength tests*

#### *3.3.1 Effect of initial moisture content on Stress-strain behaviour*

The typical stress-strain curves for five xanthan gum contents at an initial moisture content $w$=30% are shown in Fig. 8. The trends of axial stress versus axial strain of xanthan gum-treated soil samples differed gradually from that of the untreated soil sample ($m_b/m_s$=

0.0%) with the increasing $m_b/m_s$ ratio, indicating that adding xanthan gum to soils provided strengthening effects. On the other hand, the xanthan gum-treated soil samples were more deformable, i.e., the peak axial strain corresponding to the peak axial stress increased from 1.67% to 5.12% as the xanthan gum content increased from 0.0% to 5.0%.

When the initial moisture content was reduced to the treated optimum $w$=26%, the xanthan gum-treated soils also had improved stress-strain behaviours (Fig. 9), however, not as prominent as those for 30% initial moisture content. This implies that using the treated optimum as an initial moisture content did not necessarily lead to the best strengthening effect. This may be due to the undesirable workability caused by insufficient water for xanthan gum-soil matrix mixing. As described in the previous section 3.2, the plastic limit of the xanthan gum-soil matrix increased as a result of increasing the xanthan gum content. Therefore, the initial moisture content of 26% was slightly larger than the plastic limit of the soil samples after they had been treated with xanthan gum at $m_b/m_s$ ratio ranging from 1.0 to 5.0% ($w_p$= 23.5 to 25.7%).

The moisture-dependent stress-strain behaviour is further illustrated in Fig. 10. For a given value of $m_b/m_s$= 1.0%, the efficiency of xanthan gum in improving the soil mechanical behaviour was intimately related to the initial moisture content. Four of the five stress-strain curves for xanthan gum-treated soils lie above the untreated soil, indicating the strengthening effect can only be obtained for a moisture content larger than 26% (treated optimum). The treated samples prepared with the untreated optimum (23%) seemed not to differ from the untreated sample. The similar phenomenon was also observed for $m_b/m_s$ = 2.0% prepared with the untreated optimum. This could be explainable that $w$=23% was even smaller than the plastic limit of the xanthan gum-treated soils, which resulted in an unthorough mixing and prevented the xanthan gum to be an efficient binder. In addition, the strength was observed to reach a maximum value of 3.47 MPa at the initial water content $w$=30%, where either a smaller value $w$=28% or a larger value $w$=32% resulted in a reduced peak axial stress. This

phenomenon indicates that there exists an ideal initial moisture content that can lead to a maximum strengthening effect.

### *3.3.2 Effect of initial moisture content on UCS*

The variation of the unconfined compression strength (UCS) defined as the peak axial stress, with an increasing initial moisture content for untreated soils are shown in Fig. 11. The UCS underwent an increase and then a decrease as the initial moisture content increased from 17% to 30% with a peak value of 1.98 MPa at the optimum moisture content $w$=23%.

Figure 12 shows the trends of UCS with an increasing moisture content for five biopolymer contents. For a given value of $m_b/m_s$=1.0%, the UCS initially increased from 2.67 MPa to a peak value of 3.42 MPa as the initial moisture content increased from 26% to 30%. Afterwards, additional amount of water led to a reduced UCS value of 2.98 MPa. This trend retained when $m_b/m_s$ =1.0% was replaced with $m_b/m_s$ =4.0% and 5.0%. For $m_b/m_s$= 2.0% and 3.0%, the UCS values also underwent an increment and a decrement with the increasing moisture content, but the peak value of UCS was observed at $w$=28%.

The overall trend of UCS indicate that xanthan gum-treated soil samples with all five biopolymer contents grained strength as the moisture content increased from 26% to 28%. Further elevating the moisture content from 28% to 30% led to an increased UCS for $m_b/m_s$ =1.0%, 4.0% and 5.0% and a decreased UCS for $m_b/m_s$ =2.0% and 3.0%. Afterwards, as the moisture content exceeded 30%, the UCS values decreased regardless of the xanthan gum content. Therefore, the ideal initial moisture content corresponding to the maximum UCS for a given biopolymer content can be assumed to lie between 28% and 30%, which is 1.1 to 1.2 times the treated optimum.

The maximum UCS values for various biopolymer contents denoted by solid circles are extracted from Fig. 12 and shown in Fig. 13. Increasing the biopolymer content was effective

in enhancing the soil strength at the ideal initial moisture contents. The dosage of $m_b/m_s$ =1.0% increased the maximum UCS from 1.98 to 3.42 MPa, by 72%. As the biopolymer content further increased, the maximum UCS increased gradually and reached 4.36 MPa at $m_b/m_s$ =5.0% , by 115%.

The SEM images of the untreated soils and xanthan gum-treated soils ($m_b/m_s$=1.5% and $w$=28%) are presented in Fig. 14. It is clear that the xanthan gum-treated soils were less porous than the untreated soils on all three magnifications. This phenomenon is in line with the strength improvement. However, the SEM images for xanthan gum-treated Shanghai clay does not show inter-particle behaviour, e.g., clear biopolymer coating around the single soil particle and bridges between the detached soil particles, which is very common in the SEM images for the biopolymer-treated sands [13, 14, 18, 26]. The cementation mechanism for xanthan gum in Shanghai clay can be explained by the biopolymer-particle interaction. As xanthan gum is negatively charged, the existence of natural cations (e.g., $K^+$, $Ca^{2+}$, $Mg^{2+}$, and $Na^+$ in Fig. 3) in Shanghai clay promoted the ionic bonding between xanthan gum and Shanghai clay. In addition, the carboxylic acid (–COOH) and hydroxyl groups (–OH) of xanthan gum can easily induce hydrogen bonding [26]. The similar SEM observations for the biopolymer-treated fine soils can be found in [13, 47, 48].

### *3.4 Results of fatigue loading tests*

The fatigue life, which is the number of cycles at failure in the constant-amplitude fatigue loading tests for the samples with different xanthan gum contents, are given in Table 3. For the samples with $m_b/m_s$= 1.0% and $\sigma_m$/UCS =0.4, increasing the stress amplitude from $\sigma_a$/UCS = 0.15 to 0.3 led to a decreased fatigue life from 1,256,247 to 377,524 cycles. For the samples with $m_b/m_s$= 2.0% and $\sigma_a$/UCS= 0.15, a reduction in fatigue life from 1,945,328 to 525,271 cycles accompanied with an increment in $\sigma_m$/UCS from 0.4 to 0.6. Results from samples with $m_b/m_s$= 1.0% and $m_b/m_s$= 2.0% indicated that increasing either mean stress or stress amplitude, incurred more serious sample damage. To identify if mean stress or stress

amplitude played a more important role in the fatigue life of the xanthan gum-treated soil samples, the samples with $m_b/m_s$= 3.0% were designed to be exposed to identical $\sigma_{max}$/UCS= 0.7, but different components. It appeared that the soil was likely to have a short fatigue life with a higher ratio of $\sigma_m$/UCS for a given ratio of $\sigma_{max}$/UCS.

Furthermore, in Fig. 15, it is clear that the use of xanthan gum increased the fatigue life. For $\sigma_{max}$/UCS= 0.55, the untreated soil sample failed at 233,750 cycles, while the xanthan gum-treated soil sample with $m_b/m_s$= 1.0% failed at 1,256,247. When the $m_b/m_s$ ratio increased to 2.0%, the sample almost sustained till the end of the test. For $\sigma_{max}$/UCS= 0.70 and $\sigma_{max}$/UCS= 0.75, similar trends were observed.

For stepping-amplitude fatigue loading tests, all samples were subjected to a mean stress $\sigma_m$/UCS= 0.45 and repeated stresses increasing from $\sigma_a$/UCS= 0.05 to 0.35, at an interval of 0.1. Results of the fatigue life are given in Table 4. With the increment in $m_b/m_s$, the samples underwent more loading steps. The untreated soil sample failed under $\sigma_{max}$/UCS= 0.60 at the second step, while the sample with $m_b/m_s$= 1.0% failed under $\sigma_{max}$/UCS= 0.70, at the third step. The sample with $m_b/m_s$= 3.0%, although failed at the same loading step as the sample with $m_b/m_s$= 2.0%, had a longer fatigue life 215,869 cycles under $\sigma_{max}$/UCS= 0.80 compared to 95,547 cycles for $m_b/m_s$= 2.0%.

Results from the two types of the fatigue loading tests revealed a common phenomenon. The untreated soil failed under a stress level approximately half of the UCS (e.g., $\sigma_{max}$/UCS= 0.55 to 0.6), while the xanthan gum-treated soil with $m_b/m_s$= 3.0% sustained. With the increasing xanthan gum contents, the fatigue life increased regardless of the loading schemes.

### *3.5 Possible implementations of xanthan gum in geotechnical engineering practices*

Although this is a laboratory study, how soft clays can be treated with xanthan gum in practice is briefly discussed as follows.

The incorporation of xanthan gum into soils on site can be conducted through deep mixing, spraying, grouting, high-pressure injection, and etc. [9, 31, 49]. Given the high viscosity of xanthan gum solution that is prone to block the voids in soils for further solution penetration, deep mixing might be recommended. In the existing laboratory research, biopolymers have been introduced into the soil in power or solution form (i.e., dry mixing or wet mixing). According to Arab et al. [50], wet mixing method is more effective in treating different cohesive soils with sodium alginate. Ayeldeen et al. [14] observed that the efficiency of xanthan gum or guar gum through wet mixing in reducing collapsibility was about 2-3 times more than dry mixing, while Chang et al. [26] reported that dry mixing is more effective than wet mixing by providing a well-distributed xanthan matrix in soil given that the amount of mixing water is sufficient for xanthan gum dissolution. As for practical applications, dry mixing is considered as an appropriate method [51]. Therefore, the choice of mixing method in practice may need to be determined according to the solubility, the addition amount and types of biopolymers, and soil types. Furthermore, various factors such as workability, construction cost, relevant machinery, and environmental issue need to be assessed for practical and economic application on site.

## 4. Conclusions

The incorporation of xanthan gum in treating Shanghai clay was experimentally studied by performing standard proctor compaction tests, Atterberg limit tests, unconfined compression, fatigue loading tests (constant-amplitude and stepping-amplitude) and microscopic analysis. Results indicated that the initial moisture content played an important role in the effectiveness of soil treatment with xanthan gum. As the initial moisture content increased from the treated optimum 26% (3% wet of the untreated optimum), the unconfined compression strength increased until a inflection point was reached, indicting an ideal initial moisture content of 1.1 to 1.2 times the treated optimum to achieve a maximum strengthening efficiency, for all five xanthan gum contents from 1.0% to 5.0%. Furthermore, either

constant-amplitude or stepping-amplitude fatigue loading tests provided evidence that xanthan gum, as a eco-friendly soil strengthener, was efficient in increasing either soil bearing capacity or fatigue life, under repeated loads.

## Acknowledgments

The work described in this paper was supported by the National Natural Science Foundation of China (51608323, 51678319, 51978533). In addition, this project has received funding from the European Union's Horizon 2020 Framework programme Marie Skłodowska-Curie Individual Fellowships under grant agreement No. 897701 and Marie Skłodowska-Curie Actions Research and Innovation Staff Exchange (RISE) under grant agreement No. 778360.

## References

[1] J.K. Mitchell, J.C. Santamarina, Biological considerations in geotechnical Engineering, J. Geotech. Geoenviron. Eng. 131 (10) (2005) 1222–1233.

[2] J.T. DeJong, K. Soga, E. Kavazanjian, S. Burns, L.A. Van PaasseN, A. Al Qabany, A. Aydilek, S.S. Bang, M. Burbank, L.F. Caslake, C.Y. Chen, X. Cheng, J. Chu, S. Ciurli, A. Esnault-Filet, S. Fauriel, N. Hamdan, T. Hata, Y. Inagaki, S. Jefferis, M. Kuo, L. Laloui, J. Larrahondo, D.A.C. Manning, B. Martinez, B.M. Montoya, D.C. Nelson, A. Palomino, P. Renforth, J.C. Santamarina, E.A. Seagren, B. Tanyu, M. Tsesarsky, T. Weaver, Biogeochemical processes and geotechnical applications: progress, opportunities and challenges, Géotechnique 63 (4) (2013) 287–301.

[3] J.T. DeJong, M.B. Fritzges, K. Nüsslein, Microbially induced cementation to control sand response to undrained shear, J. Geotech. Geoenviron. Eng. 132 (11) (2006) 1381-1392.

[4] L. Cheng, R. Cord-Ruwisch, M.A. Shahin, Cementation of sand soil by microbially induced calcite precipitation at various degrees of saturation, Can. Geotech. J. 50 (2013) 81–90.

[5] A.A. Qabany, K. Soga, Effect of chemical treatment used in MICP on engineering properties of cemented soils, Géotechnique 63 (4) (2013) 331–339.

[6] C. He, J. Chu, Undrained responses of microbially desaturated sand under monotonic loading, J. Geotech. Geoenviron. Eng. 140 (5) (2014) 04014003.

[7] D. Terzis, R. Bernier-Latmani, L. Laloui, Fabric characteristics and mechanical response of bio-improved sand to various treatment conditions, Géotechnique Lett. 6 (2016) 50–57.

[8] P. Xiao, H.L. Liu, Y. Xiao, A.W. Stuedlein, T.M. Evans, Liquefaction resistance of bio-cemented calcareous sand, Soil Dyn. Earthq. Eng. 107 (2018) 9–19.

[9] I. Chang, J. Im, G.C. Cho, Introduction of microbial biopolymers in soil treatment for future environmentally-friendly and sustainable geotechnical engineering, Sustainability 8 (3) (2016) 251.

[10] S.M. Viswanath, S.J. Booth, P.N. Hughes, C.E. Augarde, C. Perlot, A.W. Bruno, D. Gallipoli, Mechanical properties of biopolymer-stabilised soil-based construction materials, Géotechnique Lett. 7 (4) (2017) 309–314.

[11] N.G. Reddy, B.H. Rao, K.R. Reddy, Biopolymer amendment for mitigating dispersive characteristics of red mud waste, Géotechnique Lett. 8 (3) (2018) 201-207.

[12] C. Chen, L. Wu, M. Perdjon, X. Huang, Y. Peng, The drying effect on xanthan gum biopolymer treated sandy soil shear strength, Constr. Build. Mater. 197 (2019) 271–279.

[13] I. Chang, G.C. Cho, Strengthening of Korean residual soil with $\beta$-1, 3/1, 6-glucan biopolymer, Constr. Build. Mater. 30 (2012) 30–35.

[14] M.K. Ayeldeen, A.M. Negm, M.A. El Sawwaf, Evaluating the physical characteristics of biopolymer/soil mixtures, Arab. J. Geosci. 9 (2016) 371.

[15] H.R. Khatami, B.C. O'Kelly, Improving mechanical properties of sand using biopolymers, J. Geotech. Geoenviron. Eng. 139 (2013) 1402–1406.

[16] I. Chang, A.K. Prasidhi, J. Im, G.C, Cho. Soil strengthening using thermo-gelation biopolymers, Constr. Build. Mater. 77 (2015) 430–438.

[17] I. Chang, J. Im, G.C. Cho, Geotechnical engineering behaviors of gellan gum treated sand, Can. Geotech. J. 53 (2016) 1658-1670.

[18] I. Chang, J. Im, S.W. Lee, G.C. Cho, Strength durability of gellan gum biopolymer-treated Korean sand with cyclic wetting and drying, Constr. Build. Mater. 143 (2017) 210–221.

[19] I. Chang, G.C. Cho, Shear strength behavior and parameters of microbial gellan gum-treated soils: from sand to clay, Acta. Geotech. 14 (2019) 361–375.

[20] R. Aguilar, J. Nakamatsu, E. Ramírez, M. Elgegren, J. Ayarza, S. Kim, M.A. Pando, L.

Ortega-San-Martin, The potential use of chitosan as a biopolymer additive for enhanced mechanical properties and water resistance of earthen construction, Constr. Build. Mater. 114 (2016) 625–637.

[21] N. Hataf, P. Ghadir, N. Ranjbar, Investigation of soil stabilization using chitosan biopolymer, J. Clean Prod. 170 (2018) 1493–1500.

[22] J. Nakamatsu , S. Kim, J. Ayarza, E. Ramírez, M. Elgegren, R. Aguilar, Eco-friendly modification of earthen construction with carrageenan: Water durability and mechanical assessment, Constr. Build. Mater. 139 (2017) 193–202.

[23] H. Fatehi, S.M. Abtahi, H. Hashemolhosseini, S.M. Hejazi, A novel study on using protein-based biopolymers in soil strengthening, Constr. Build. Mater. 167 (2018) 813–821.

[24] I. Chang, J. Im, M.K. Chung, G.C. Cho, Bovine casein as a new soil strengthening binder from diary wastes, Constr. Build. Mater. 160 (2018) 1–9.

[25] P. Ghadir, N. Ranjbar, Clayey soil stabilization using geopolymer and Portland cement, Constr. Build. Mater. 188 (2018) 361-371.

[26] I. Chang, J. Im, A.K. Prasidhi, G.C. Cho, Effects of xanthan gum biopolymer on soil strengthening, Constr. Build. Mater. 74 (2015) 65–72.

[27] N. Latifi, S. Horpibulsuk, C.L. Meehan, M.Z.A. Majid, A.S.A. Rashid, Xanthan gum biopolymer: an eco-friendly additive for stabilization of tropical organic peat, Environ. Earth. Sci. 75 (2016) 825.

[28] G.C. Barrére, C.E. Barber, M.J. Daniels, Molecular cloning of genes involved in the production of the extracellular polysaccharide xanthan by *Xanthomonas campestris* pv. *campestris*, Int. J. Biol. Macromol. 8 (1986) 372–374.

[29] S. Rosalam, R. England, Review of xanthan gum production from unmodified starches by xanthomonas comprestris sp, Enzyme Microb. Technol. 39 (2) (2006) 197–207.

[30] C. Lam, S.A. Jefferis, The use of polymer solutions for deep excavations: lessons from Far Eastern experience. HKIE Transactions 21 (4) (2014) 262-271.

[31] C. Lam, S.A. Jefferis, Polymer Support Fluids in Civil Engineering, ICE, 2017.

[32] R. Guerrero-Lemus, J.M. Martinez-Duart, Renewable energies and $CO_2$: Cost Analysis, Environmental Impacts and Technological Trends, 2012 edition, Springer London, UK, 2013.

[33] H.B. Seed, C.K. Chan, Clay strength under earthquake loading conditions, J. Soil Mech. Found. Div. 92 (2) (1966) 53–78.

[34] J.P. Carter, J.R. Booker, C.P. Wroth, A critical state soil model for cyclic loading, Soil mechanics—Transient and cyclic loading (1982) 219–252.

[35] J.C. Chai, N. Miura, Traffic-load-induced permanent deformation of road on soft subsoil, J. Geotech. Geoenviron. Eng. 128 (11) (2002) 907–916.

[36] X. Geng, C. Xu, Y. Cai, Non-linear consolidation analysis of soil with variable compressibility and permeability under cyclic loadings, Int. J. Numer. Anal. Met. 30 (8) (2006) 803–821.

[37] K.H. Andersen, Bearing capacity under cyclic loading—offshore, along the coast, and on land, Can. Geotech. J. 46 (5) (2007) 513–535.

[38] J. Ni, I. Indraratna, X. Geng, J.P. Carter, Y. Chen, Model of soft soils under cyclic loading, Int. J. Geomech. 15 (4) (2015) 04014067 (10 pp.).

[39] Y. Cai, X. Geng, C. Xu, Solution of one-dimensional finite-strain consolidation of soil with variable compressibility under cyclic loadings, Comput. Geotech. 34 (1) (2007) 31-40.

[40] Y. Cai, X. Geng, Consolidation analysis of a semi-infinite transversely isotropic saturated soil under general time-varying loadings, Comput. Geotech. 36 (3) (2009) 484-492.

[41] J. Wang, Z. Gao, H. Fu, G. Ding, Y. Cai, X. Geng, C. Shi, Effect of surcharge loading rate and mobilized load ratio on the performance of vacuum–surcharge preloading with PVDs, Geotext. Geomembranes 47 (2) (2019) 121-127

[42] Y. Chen, J. Ni, P. Zheng, R. Azzam, Y. Zhou, W. Shao, Experimental research on the behaviour of high frequency fatigue in concrete, Eng. Fail Anal. 18 (2011) 1848–1857.

[43] Y. Chen, J. Ni, W. Shao, Y. Zhou, A. Javadi, R. Azzam, Coalescence of fractures under uni-axial compression and fatigue loading, Rock Mech. Rock. Eng. 45 (2012a) 241–249.

[44] Y. Chen, J. Ni, W. Shao, R. Azzam, Experimental study on the influence of temperature on the mechanical properties of granite under uni-axial compression and fatigue loading, Int. J. Rock Mech. Min. 56 (2012b) 62–66.

[45] B.M. Lekha, G. Sarang, A.U.R. Shankar, Effect of electrolyte lignin and fly ash in stabilizing black cotton soil, Transp. Infrastruct. Geotech. 2 (2015) 87–101.

[46] I. Chang, Y.M. Kwon, J. Im, G.C. Cho, Soil consistency and interparticle characteristics of xanthan gum biopolymer – containing soils with pore-fluid variation, Can. Geotech. J. 56 (8) (2019) 1206–1213.

[47] A. Soldo, M. Miletić, M.L. Auad, Biopolymers as a sustainable solution for the enhancement of soil mechanical properties, Sci. Rep-Uk. 10 (1) (2020) 213-267.

[48] A.S.A. Rashid, S. Tabatabaei, S. Horpibulsuk, N.Z. Mohd Yunus, W.H.W. Hassan, Shear Strength Improvement of Lateritic Soil Stabilized by Biopolymer Based Stabilizer, Geotechnical and Geological Engineering 37 (6) (2019) 5533-5541.

[49] S. Smitha, K. Rangaswamy, D.S. Keerthi, Triaxial test behaviour of silty sands treated with agar biopolymer, International Journal of Geotechnical Engineering (2019) 1-12.

[50] M.G. Arab, A.M. ASCE, R.A. Mousa, A.R. Gabr, A.M. Azam, S.M. El-Badawy, A.F. Hassan, Resilient behavior of sodium alginate – treated cohesive soils for pavement applications, J. Mater. Civ. Eng. 91 (3) (2019) 04018361.

[51] A.F. Cabalar, M.H. Awraheem, M.M. Khalaf, Geotechnical properties of a low-plasticity clay with biopolymer, J. Mater. Civ. Eng. 30 (8) (2018) 4018170.